Theoretical modelling of temporal compression of optical pulses and pulse sequences using photon echoes.

Mikael Afzelius

Master Thesis,
LRAP 251, LTH/LU, 1999

LUND
UNIVERSITY

Abstract

In recent years possible applications of the photon echo process in optical processing, data storage systems, bit-rate conversion of optical pulses, time compression of optical pulses etc. have been investigated. Much of this research aim at replacing electrical components in the framework of today's information networks with components that are entirely based on optics. It is likely that we in the future will see more and more of the electrical components linked to a fibre network being replaced by all optical components, e.g. routers and bit-rate converters. The concept of temporal compression of optical pulses, which is the subject of this thesis, could be used to increase the transmission rate through optical fibres and thereby use the full capacity of today's fibres. It should also be mentioned that more basic components, e.g. XOR gates, are studied in this research field and these components could possibly be used in future concepts of a "light-computer".

In this thesis a theoretical model of time compression of both single optical pulses and optical pulse sequences using photon echoes is presented. A full analytical treatment was done for gaussian shaped pulses as a first step of building a numerical model. An analytic approximate approach was also used for both square pulses and pulse sequences. A theoretical understanding of the duration, the intensity spectrum and peak intensity of the compressed signals was reached. It is shown that the intensity spectrum of a compressed pulse sequence containing N bits is completely analogous to the pattern observed in the well-known Fraunhofer diffraction experiment with N slits.

A numerical model was built and used to evaluate how non-linearities and noise affect the degree of compression. In addition theoretical models were developed to explain the effects of non-linearities and noise and the hope is that these might be used as guidelines on how to design future experiments in order to achieve highest possible degree of compression. Some of the results presented in this thesis is compared with experimental data obtained in the research group during the time this work was going on.

Contents

1 Introduction

In the Photon Echo group at the Division of Atomic Physics (Lund Institute of Technology) there is a project, supported by the TFR (Teknikvetenskapliga Forskningsrådet), that among other things aim at investigating a concept for increasing the transmission rate in optical fibres using the photon echo process [1].
The scheme is to send in an optical pulse sequence into a photon echo material to compress the signal in time. The compressed signal is transmitted through an optical fibre and in the other end a reversed photon echo process decompresses the signal to its original duration. A reason for doing this is that today the transmission rate in optical fibres are limited to a few hundred GHz, while the fibre itself is capable of THz rate, and the hope is to bridge this gap with the described process.
Several experiments performed in laboratories around the world, and in the Photon Echo group here, has shown that time compression of an optical pulse using photon echoes is possible [2,3,4,5] . Compression in combination with the inverse process has not been performed yet, because in a typical photon echo experiment the compressed signal has a peak intensity of only 0.1 –1 % of the input pulse intensities. Much work is put into an experiment in the group to develop a fibre amplifier that could amplify the compressed signal a factor of 100 – 1000, which probably would be enough to compensate for the intensity loss in the photon echo process.
The purpose of this thesis is to theoretically examine the properties of the compression and decompression processes utilising the photon echo process. In short, a photon echo is a non-linear process where two/three optical pulses are sent into a photon echo material and an optical response, the photon echo, is emitted. In the scheme above, the first pulse would be the pulse sequence and the second pulse would perform the compression in time. This is feasible if the two pulses both are frequency chirped over identical and sufficiently large frequency intervals and the second pulse has half the duration of the first one.
I have made a complete analytical calculation assuming that the excitation pulses are gaussian shaped in time and also an approximate solution for square shaped pulses, under the conditions that apply for compression. Then a numerical model was built for both square and gaussian pulses where the analytic calculation for the gaussian case was used to check the correctness of the programs. This approach minimise the risk for errors while making the numerical programs.
The work focused on the temporal appearance of the echo, e.g. the duration of the compressed pulse sequence, for both simple input pulses and arbitrary pulse sequences. The intensity as a function of chirp widths and pulse lengths was examined, however the absolute intensity depend on variables specific for a certain photon echo material and these issues have been outside the scope of this work. We especially wanted to know the requirements on an experimental system in order to maximise the compression and be able to faithfully reconstruct the data later. The issues that has been delt with in connection with this has mainly involved the relationship between the chirps over the two pulses, what temporal portion of the echo is needed for decompression and the influence of phase noise in the laser radiation.
In Chapter 2 the basic theory of photon echoes is explained, which serve as a foundation for the following chapters. The analytical calculations are made in Chapter 3, while the numerical calculations are explained in Chapter 4. The analytical results are verified in Chapter 5 by comparing with the numerical model and in Chapter 6 I make some comparisons with experimental data from experiments performed by Xiangjun Wang, a diploma worker in the same group. In the last chapter the results are discussed.

2 Theory of photon echoes

2.1 Overview

First of all, the photon echo is a result from the coherent interaction between light and a medium. Most light matter interaction processes are linear in the incoming fields, e.g. reflection and refraction, but when the light has sufficiently high intensity or the excitation is resonant with an atomic transition, as is the case in these photon echo experiments, the response of the medium can be a non-linear function of the incoming electromagnetic field. Photon echoes can be viewed as a four-wave mixing process. In four-wave mixing three electromagnetic fields interact simultaneously with the material and their combined interaction with the material produces a fourth field. However, in a photon echo process the incoming fields can also be separated in time and still yield a fourth output field, a consequence of the special properties of the materials in use (more about this later). Thus, a photon echo is a process where light pulses are sent into a material at different times and an optical response is emitted at a later time. As in four-wave mixing, three input fields will produce a fourth field. It is also possible to get an echo from two fields where the second field simultaneously acts as the second and third field in the three-pulse case. In this thesis I will only deal with the two-pulse photon echo process (Figure 2.1.1).

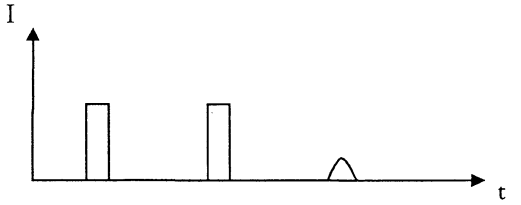

Figure 2.1.1. In a two-pulse photon echo process two input pulses interact with the material at different times. Their combined interaction with the material generate an optical response or echo after a time interval that corresponds to the time difference between the input pulses.

2.2 Quantum mechanical description

The processes responsible for the photon echo can be understood by a quite simple semi-classical model [6], where the atom is quantised but the interacting light is treated as a classical plane wave. I will show some state equations for the atom and the main principle behind the optical response, the "phase reversal", by evaluating the amplitudes of the eigenstates as a function of time. Assume that the atom is a two level system with energy levels zero and $E = \hbar\omega$. The state of the atom, denoted $|t\rangle$, can be written as a linear combination of the energy states $|a\rangle$ and $|b\rangle$ of energies 0 and E with some amplitudes $a(t)$ and $b(t)$, and a phase factor in the upper state due to the energy difference between the states:

$$|t\rangle = a(t)|a\rangle + e^{-i\omega t}b(t)|b\rangle. \qquad (2.2.1)$$

The magnitude of the amplitudes squared, $|a(t)|^2$ and $|b(t)|^2$, are the possibilities to find the atom in state $|a\rangle$ and state $|b\rangle$ respectively, these have to fulfil $|a(t)|^2 + |b(t)|^2 = 1$ at all times (conservation of probability). Assume that all the atoms are in the ground state at time $t = 0$, i.e. $a(0) = 1$ and $b(0) = 0$, and that they interact with a plane wave of laser light starting at time $t = 0$. The laser pulse is expressed as:

$$E(\bar{r},t) = Ee^{-i\omega_0 t}e^{-i\bar{k}\cdot\bar{r}}. \qquad (2.2.2)$$

The light has the angular frequency ω_0 and the direction of propagation $\bar{k}$. I will not go into detail how this interaction is treated quantum mechanically, but essentially the amplitudes $a(t)$ and $b(t)$ change during the interaction. If the light pulse has length t_1 the final amplitudes after the interaction time t_1 becomes:

$$a(t_1) = \cos\theta/2$$
$$b(t_1) = ie^{i\bar{k}\cdot\bar{r}}\sin\theta/2 \qquad (2.2.3)$$

Here, the *pulse area* θ is defined as (μ is the electric dipole transition moment of the $|a\rangle$ to $|b\rangle$ transition in the atom)

$$\theta = \frac{E\cdot t_1\cdot\mu}{\hbar}. \qquad (2.2.4)$$

One can easily see that after a pulse with pulse area $\theta = \pi/2$ an atom has 50% probability to be in the upper state, i.e. $|a(t_1)|^2 = |b(t_1)|^2 = 1/2$.

The macroscopic polarisation of the material is the sum of the individual electric dipole transition moments caused by the single atoms. The expectation value of a dipole transition moment for an atom is:

$$P_a = \langle t|\hat{\mu}|t\rangle, \qquad (2.2.5)$$

where $\hat{\mu}$ is the quantum operator for the electric dipole transition moment of the atom.

After the first pulse the atoms start to emit radiation because the macroscopic polarisation oscillates at the frequency of the light. All the atomic dipoles are, at time t_1, in phase because all atoms interact with the same plane wave. The excited atoms will however at later times gain phase relative to the ground state atoms because of the phase factor in Equation (2.2.1). This phase factor $e^{-i\omega(t-t_1)}$ also propagate to the expression for the dipole moment, Equation (2.2.5), hence the individual dipole moments oscillate at angular frequency ω.
It is time to mention a very important property of the materials being used in these processes. It is well known that processes as collisions between particles in a gas homogeneously broaden the resonance frequency of an atomic level. Another broadening mechanism, inhomogeneous broadening, takes place on a larger scale and may contain many homogeneously broadened resonance frequencies (Figure 2.2.1). Inhomogeneous broadening in a crystal for example, is a result of imperfections and local variations in the lattice. These imperfections shift the resonance frequencies.

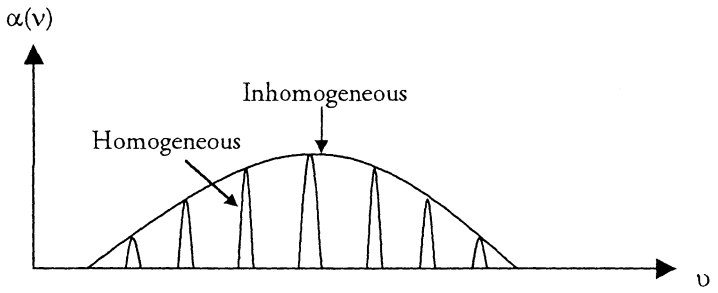

Figure 2.2.1. This is the absorption coefficient $\alpha(\nu)$ as a function of frequency. The wide absorption profile caused by inhomogeneous broadening might contain several millions of homogeneously broadened resonance frequencies.

If the pulse above excites atoms within an interval of the inhomogeneous broadening that contains several individual homogeneous components, the radiation emitted is generated by dipole moments with different phase factors. As a result, the atoms at different resonance frequencies will quickly dephase with respect to each other. This is called the *free-induction decay*. Right after the pulse they are in phase and the fields add up coherently, which has the effect that the total intensity is proportional to the number of atoms squared, N^2. As the dipole moments start to dephase, the fields do not add up coherently anymore and the intensity is instead proportional to the number of atoms.
The next step is to send in a second pulse of length t_2 a time τ after the first pulse. The excited atoms at one resonance frequency ω have then gained a phase factor $e^{-i\omega\tau}$ relative to the lower lever. The second pulse de-excites some of the upper state atoms and excites some of the lower state atoms. These atoms keep their phase relation, that is the de-excited atoms are now "ahead" in phase relative the excited atoms, this important feature is called *phase reversal*. The amplitude terms of the excited/de-excited atoms after the second pulse, at time $t_1+\tau+t_2$, is:

$$\begin{aligned} a(t_1+\tau+t_2) &= -\sin(\theta_1/2)\sin(\theta_2/2)e^{-i\omega t} \\ b(t_1+\tau+t_2) &= i\sin(\theta_2/2)\cos(\theta_1/2)e^{i\bar{k}\cdot\bar{r}} \end{aligned} \quad , \qquad (2.2.6)$$

where θ_1 and θ_2 are the pulse areas of pulse one and two respectivly.
Since the upper state atoms will gain phase again, the excited atoms will have the same phase as the de-excited atoms after another time-interval τ. This is true for all the atoms within the inhomogeneous broadening. Again the fields add up coherently (the individual dipole

transition moments from Equation (2.2.5) will be in phase) and the intensity of the light raise by a factor N. This is the echo! To calculate the total intensity one has to integrate over all excited frequencies in the inhomogeneous broadening, which can be described by some distribution function. This calculation is specific to the kind of material in use, e.g. crystal or gas.
It is crucial that the atoms keep their phase relation during the experiment. One could say that the material should have a long *phase memory*. This property is destroyed when particles in a gas collide or by phonons in a crystal. When crystals are used as photon echo material they are cooled down to liquid helium temperatures to minimise any disturbances that could cause the atoms to lose their phase memory. In the following we disregard any such processes that would destroy the photon echo.

2.3 Fourier model

The quantum mechanical description in section 2.2 explains the underlying processes that cause an optical response from the medium, but it is not very useful for an analytic treatment of complicated experiments, for example if the input pulses are frequency chirped. For this purpose it is better to use an alternative description based on Fourier transforms of the input pulses. The following discussion is based on a PhD thesis made at the department [7].

Looking at the polarisation P of the material when subject to three input pulses can motivate this approach. For most purposes the polarisation is linear in the applied field, but generally the polarisation has non-linear terms:

$$P = \varepsilon_0\left(\chi_1 E(\omega) + \chi_2 E(\omega)^2 + \chi_3 E(\omega)^3 + \chi_4 E(\omega)^4 + \ldots\right) \qquad (2.3.1)$$

The optical response of a certain order depends on the corresponding susceptibility χ_i and the electric field strength. The second and third order susceptibilities are several orders of magnitude lower than the linear susceptibility, which in many materials is unity. To see the second and third order non-linear effects the input field strength have to be large enough or alternatively the excitation can be performed at resonance using a coherent field. In either case a laser is most commonly used. The photon echo is a third order process and generally the peak intensity of the echo is at best 0.1 – 1 % of the input intensities. The polarisation in the third order can be expressed as:

$$P^{(3)} = \varepsilon_0 \chi_3 E(\omega)^3 \qquad (2.3.2)$$

Denote the electric field of the three incoming pulses as E_1, E_2, E_3 (in that time-order) and let $E_i = \widetilde{E}_i + \widetilde{E}_i^*$ ($\widetilde{E}$ is a complex quantity describing the light pulses). Evaluate Equation (2.3.2):

$$P^{(3)} = \chi_3(\widetilde{E}_1^*\widetilde{E}_2\widetilde{E}_3 + \ldots. + \widetilde{E}_1^*\widetilde{E}_2^2 + \ldots) \qquad (2.3.3)$$

I have only written out two terms in this sum, the ones corresponding to a three pulse photon echo between all the three pulses and a two photon echo between pulse one and two. The conjugation of one factor in each term can be understood by phase matching. The wavevector of the output pulse $\bar{k}_e$ is a linear combination of the wavevectors of the input pulses $\bar{k}_i$. Assume that all the pulses have the same wavelength and that the excitation is collinear, i.e. $\bar{k}_e = \bar{k}_1 = \bar{k}_2 = \bar{k}_3$, then the following relationship is always fulfilled:

$$\bar{k}_e = \bar{k}_3 + \bar{k}_2 - \bar{k}_1 \qquad (2.3.4)$$

This indicates that one of the pulses should be conjugated and one can show that this ought to be the first pulse, otherwise causality is violated when the inverse Fourier transform is made of the third order polarisation (this gives the echo as a function of time).
The discussion above is only an indication of how the photon echo process can be treated by Fourier transforms. To express the echo as a function of time, Fourier transform the input pulses, i.e. transform the electric field from a function in time $E(t)$ to a function in frequency $E(\omega)$, calculate $E(\omega)_1^* E(\omega)_2 E(\omega)_3$ (or $E(\omega)_1^* E(\omega)_2^2$ in case of two-pulse echo) and make the

inverse transform. This method is the foundation of the calculations made in this thesis, both numerical and analytical. Finally, the two-pulse photon echo as a function of time can be written as [7, 8]:

$$E(t) = \frac{2\mu^2 L}{\hbar^2} \int_{-\infty}^{\infty} E(\omega)_1^* \cdot E(\omega)_2^2 \alpha(\omega) e^{i\omega t} d\omega \,. \tag{2.3.5}$$

Here μ is the atomic dipole transition moment of the absorbers, L the length of the medium and $\alpha(\omega)$ the absorption coefficient expressed as:

$$\alpha(\omega) = \frac{4\pi^2 N g(\omega) \omega \mu^2}{\hbar c}, \tag{2.3.6}$$

where N is the density of absorbers in the medium and $g(\omega)$ is a normalised distribution function describing the inhomogeneous absorption profile. If the excitation pulses only excite atoms throughout a portion of the inhomogeneous broadening, $\alpha(\omega)$ in Equation (2.3.5) can be regarded as a constant. In the following chapters I will not deal with the absolute value of the echo, since the constants above are pretty troublesome to calculate and moreover specific for the medium used. I will instead refer to the following simplified relation:

$$E(t) \propto \int_{-\infty}^{\infty} E(\omega)_1^* \cdot E(\omega)_2^2 e^{i\omega t} d\omega \,. \tag{2.3.7}$$

In time domain this can be expressed as:

$$E(t) \propto E_1(t) \otimes E_2(t) * E_2(t), \tag{2.3.8}$$

which is the correlation of the second field with itself, convoluted with the first field.

3 Analytic treatment

3.1 Temporal compression using photon echoes

The photon echo phenomena has only been discussed generally so far and one can use this phenomena in various situations in atomic physics. This master thesis is however intended to study the application of photon echoes to compress an optical signal in time. In this section the main principles for this experiment will be outlined and the following sections in this chapter will in detail discuss requirements and limitations for such a process.

For some time, the possibility to use the photon echo process to compress optical signals in time has been discussed in several papers. The general idea is to send an amplitude-modulated signal through a crystal, the signal could be some binary pulse sequence that is going into an optical fibre, and then send in a second pulse to compress the sequence to a very short signal, which would be emitted as the echo. It turns out that if the two pulses are chirped over a large frequency interval, the resulting echo can be made much briefer than the original pulses.

The principles of time compression can be understood by considering two pulses of length T and $T/2$, chirped over the same frequency interval and separated by a time τ. An important property of photon echo is the "time memory", that is if you send in two (unchirped) pulses separated by some time τ, the optical response is emitted a time τ after the second pulse. When the pulses are chirped, atoms excited by each small frequency segment in the first pulse will interact with the corresponding frequency segment in the second pulse and at a time τ_{int} after the second interaction, where τ_{int} is the time difference between the interaction with the two frequency segments an, echo will be emitted (figure 3.1.1). All these "separate echoes" from the different individual frequency segments will be emitted at the same time and thus the echo will have a short duration. The frequency bandwidth of the echo pulse is the same as the chirp width of the excitation pulses, therefore the pulse minimum equals the inverse of this bandwidth. In the following sections the shape and intensity of the echo will be examined for gaussian and square amplitude modulated signals.

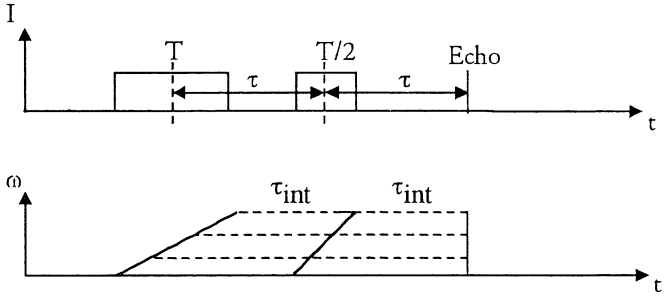

Figure 3.1.1. A schematic picture of the principle of time compression using photon echoes. The uppermost plot show the intensity of the input pulses and the echo as a function of time. The intensity of the echo is exagerated. The plot at the bottom shows the frequency spectrum as a function of time of the input pulses and the echo.
Because the second pulse is frequency chirped twice as fast as the first one, atoms with different resonance frequencies will emit radiation at the same time, even though the interaction with the material occured at different times.

3.2 Gaussian pulses

General definitions

In this section I will solve Equation (2.3.7) analytically for two chirped excitation pulses with gaussian shapes. Generally gaussian pulses are more favourable to treat analytically than square wave pulses and in this case it is even possible to find an exact solution.
The outline for solving this problem is as follows. The electrical fields for the pulses are expressed as a function of time, then a Fourier transform takes these to the frequency domain. Once the functions $E_k(\omega)$, k=1,2, are known, the inverse Fourier transform of the product $E_1^*(\omega)\cdot E_2^2(\omega)$ will give the solution for the echo. The electrical fields of the excitation pulses have the form

$$E(t) = e^{-t^2/T^2}\cdot e^{-i(\omega_0+Kt)t}\cdot e^{-i\bar{k}\cdot\bar{r}} \qquad (3.2.1)$$

where the three terms represent the amplitude, phase and spatial parts of the field. The constant T is related to the full width at half maximum (FWHM) of the intensity through

$$T_{FWHM} = \sqrt{\ln 4}\cdot T. \qquad (3.2.2)$$

If we write the phase as $\varphi = \omega_0 t + Kt^2$, where ω_0 is referred to as the *central frequency* and K is the *chirping constant*, the instantaneous frequency at time t is defined as:

$$\omega_i(t) \equiv \frac{d\varphi(t)}{dt} = \omega_0 + 2Kt. \qquad (3.2.3)$$

Assume that we chirp the pulse over an interval ω_{ch} during the time T, we would like the frequency to be $\omega_i = \omega_0 \pm \omega_{ch}/2$ at $t = \pm T/2$ and therefore define the chirping constant as:

$$K = \frac{\omega_{ch}}{2\cdot T}. \qquad (3.2.4)$$

General solution

The first step of solving integral (2.3.7) is to take the Fourier transform of the excitation pulses. In appendix A some Fourier transformation rules are given.
If the two pulses are sent into the photon echo material at different times t_1 and t_2, the electrical fields have the form $E_k(t-t_k)$, k=1,2, where $E(t)$ is of the form (3.2.1). But because of Equation (A. 3) the time constant is not important in the Fourier transformation of $E(t)$ and can be handled by taking it out of the integral. The spatial part $e^{-i\bar{k}\cdot\bar{r}}$ has no frequency or time dependence and can be considered a constant in the integral. The central frequency ω_0 can also be taken out of the integral, use Equation (A. 5), if we instead take the result as a function of $\omega+\omega_0$. The transform simplifies to:

$$E(\omega) = F[E(t-t_k)] = e^{-it_k\omega}e^{-i\bar{k}\cdot\bar{r}}\left(F\left[e^{-t^2/T^2}e^{-iKt^2}\right]\right)(\omega+\omega_0) \qquad (3.2.5)$$

The remaining problem is a standard result, Equation (A. 7),

$$E(\omega) = Ze^{-it_k\omega}e^{-i\bar{k}\cdot\bar{r}}e^{-Y(\omega+\omega_0)^2},$$

(3.2.6)

$$\text{where } Z = \sqrt{\frac{\pi \cdot T^2}{1+iKT^2}} \text{ and } Y = \frac{T^2}{4+i4KT^2}.$$

In the next step we consider two pulses at time t_1 and t_2, of length T_1 and T_2, with chirping constants K_1 and K_2 and wavenumbers k_1 and k_2. We now solve the integral describing the optical response from the photon echo material. Again the terms of the form $e^{\pm it_k\omega}$ can be taken out of the integral by use of Equation (A. 6) and we consider the remaining solution as a function of t-$2t_2$+t_1, the time when the echo occurs, Equation (A. 4) removes the variable ω_0 from the integral. We also get a spatial constant $e^{-i(2\bar{k}_2-\bar{k}_1)\cdot\bar{r}}$, which defines the direction of propagation as $2\bar{k}_2 - \bar{k}_1$. This is a very nice property of photon echoes; that one can send in excitation pulses in two different directions at different times and get a response in a third direction after a certain time. The integral reduces to:

$$E_e(t) \propto Z_1^* Z_2^2 e^{-i(2\bar{k}_2-\bar{k}_1)\cdot\bar{r}}\left(F^{-1}\left[e^{-(Y_1^*+2Y_2)\omega^2}\right]\right)(t-2t_2+t_1)e^{-i\omega_0(t-2t_2+t_1)}$$

(3.2.7)

Let $1/\chi = Y_1^* + 2Y_2$ and use Equation (A. 8) to calculate the total solution:

$$E_e(t) \propto Z_1^* Z_2^2 \sqrt{\pi \cdot \chi}\, e^{-i(2\bar{k}_2-\bar{k}_1)\cdot\bar{r}} e^{-i\omega_0(t-2t_2+t_1)} e^{-\chi\cdot(t-2t_2+t_1)^2/4}$$

(3.2.8)

$$\chi = \frac{\left(\frac{T_1^2}{4+\omega_{ch,1}^2 T_1^2} + \frac{2T_2^2}{4+\omega_{ch,2}^2 T_2^2}\right) - i\cdot\left(\frac{\omega_{ch,1}T_1^3}{8+2\omega_{ch,1}^2 T_1^2} - \frac{\omega_{ch,2}T_2^3}{4+\omega_{ch,2}^2 T_2^2}\right)}{\left(\frac{T_1^2}{4+\omega_{ch,1}^2 T_1^2} + \frac{2T_2^2}{4+\omega_{ch,2}^2 T_2^2}\right)^2 + \left(\frac{\omega_{ch,1}T_1^3}{8+2\omega_{ch,1}^2 T_1^2} - \frac{\omega_{ch,2}T_2^3}{4+\omega_{ch,2}^2 T_2^2}\right)^2}.$$

(3.2.9)

Requirement for compression

This result seems complicated and not very easy to evaluate, but there are several simplifications that one can make. We immediately see from (3.2.8) that the echo intensity will have a gaussian shape in the time domain

$$I \propto |E_e(t)|^2 \propto \left|e^{-t^2\cdot\chi/4}\right|^2 = e^{-\frac{t^2}{2}\cdot\mathrm{Re}(\chi)},$$

(3.2.10)

where we now have chosen $t_e = 2t_2 - t_1$as time zero.
The general FWHM of the echo can then be written as (3.2.2)

$$T_e = 2\sqrt{\frac{\ln 4}{\mathrm{Re}(\chi)}}.$$

(3.2.11)

Further we demand that $\omega_{ch,k} \cdot T_k >> 1$, which means that the frequency bandwidth because of the pulse length is much less than the frequency chirp over that pulse, a very reasonable

requirement for many purposes. The Re(χ) constant can under these conditions be simplified to

$$\mathrm{Re}(\chi) \approx \frac{\frac{1}{\omega_{ch,1}^2} + \frac{2}{\omega_{ch,2}^2}}{\left(\frac{1}{\omega_{ch,1}^2} + \frac{2}{\omega_{ch,2}^2}\right)^2 + \left(\frac{T_1}{2\omega_{ch,1}} - \frac{T_2}{\omega_{ch,2}}\right)^2}.$$

(3.2.12)

Maximise the expression above to find the shortest possible echo duration, that is to minimise Equation (3.2.11). We seek a configuration of T_1, T_2, $\omega_{ch,1}$ and $\omega_{ch,2}$ that maximise the above equation, let

$$\left(\frac{T_1}{2\omega_{ch,1}} - \frac{T_2}{\omega_{ch,2}}\right)^2 = 0 \Leftrightarrow \frac{\omega_{ch,2}}{T_2} = 2\frac{\omega_{ch,1}}{T_1}.$$

(3.2.13)

If we define the *chirp-rate* as $R_i = \omega_{ch,i}/T$, the requirement for optimal compression can be formulated in terms of chirp-rates:

$$R_2 = 2 \cdot R_1.$$

(3.2.14)

Already in section 3.1 we found this to be a requirement for compression and this formal treatment justify that statement.

Compression

We say that the echo is compressed whenever $R_2 > R_1$, and by maximal compression we mean that relation (3.2.14) holds for the chirp-rates of the excitation pulses. Consider two pulses of length T and $T/2$, chirped over the same interval ω_{ch}, then the condition for compression is fulfilled. We begin with writing down the FWHM of the echo, since $\mathrm{Re}(\chi) = \omega_{ch}^2/3$ and by Equation (3.2.11):

$$T_e = \frac{2\sqrt{3 \cdot \ln 4}}{\omega_{ch}} \approx \frac{4.1}{\omega_{ch}}.$$

(3.2.15)

That the length of the echo is proportional to the inverse of the chirp bandwidth is not surprising and this has also been discussed earlier and several papers have mentioned it [2,4]. Without taking into account the material constant in integral (2.3.5), nothing about the absolute intensity can be said. Nevertheless, some results about the behaviour of the intensity as a function of pulse length and chirp width can be reached. Consequently, take the squared absolute value of (3.2.8) and consider the peak value at time t=$2t_2$-t_1:

$$I_{peak} \propto \left|Z_1^* Z_2^2 \sqrt{\pi \cdot \chi}\right|^2 \propto \frac{4\pi \cdot T_1^2}{\left|4 - i\omega_{ch,1}T_1\right|}\left(\frac{4\pi \cdot T_2^2}{\left|4 + i\omega_{ch,2}T_2\right|}\right)^2 |\chi|$$

(3.2.16)

We again make the assumption that $\omega_{ch,k} \cdot T_k >> 1$ and simplify the relation above,

$$I_{peak} \propto \frac{T_1}{\omega_{ch,1}} \cdot \left(\frac{T_2}{\omega_{ch,2}} \right)^2 \cdot |\chi| \tag{3.2.17}$$

The constant χ is of the form $a/|a|^2$, why the last term in the expression above can be written as $1/|a|$ and using (3.2.9) we get the following result

$$I_{peak} \propto \frac{T_1}{\omega_{ch,1}} \cdot \left(\frac{T_2}{\omega_{ch,2}} \right)^2 \Bigg/ \sqrt{\left(\frac{1}{\omega_{ch,1}^2} + \frac{2}{\omega_{ch,2}^2} \right)^2 + \left(\frac{T_1}{2\omega_{ch,1}} - \frac{T_2}{\omega_{ch,2}} \right)^2} \,. \tag{3.2.18}$$

In the case of compression, i.e. we let the variables be related to each other as in Equation (3.2.13)with $T_1 = 2T_2$, the peak value of the intensity goes like

$$I_{peak} \propto \frac{T^3}{\omega_{ch}} \,. \tag{3.2.19}$$

3.3 Square pulses

We have seen that solving the Fourier transform based model of photon echoes with gaussian excitation pulses, gives valuable information on the requirements of compression and the shape and peak value of the intensity. However, in the experiments performed in the laboratory so far, the excitation pulses are more likely to be square shaped and therefore we make an attempt to find a solution for square pulses. Unfortunately there is no easy way to solve the transformation of a chirped square pulse between time and frequency domain. There is though a possible approach used in a paper by Graf *et al.* [2], who suggested that, in the regime $\omega_{ch} \cdot T >> 1$, the excitation pulses can be regarded as constant in the frequency interval $[\omega_0 - \omega_{ch}/2, \omega_0 + \omega_{ch}/2]$ and zero otherwise. This approximation removes the first step of Fourier transforming the excitation pulses and reduces the $E_k(\omega)$ functions to constants within that interval. In case of compression, the frequency spectrum of the echo is emitted at one instant, then a simple transformation of the product $E_1^*(\omega) \cdot E_2^2(\omega)$, that is the frequency spectrum of the echo, will give the wanted solution. If the pulses do not fulfil Equation (3.2.14), the echo will be emitted during some time interval instead and then the above approach is not possible since we assumed that the echo as a function of time was the Fourier transform of the frequency spectrum of the echo.

Consider two chirped excitation pulses of length T and $T/2$ respectively. Assume that both excitation pulses are chirped over the bandwidth ω_{ch} and that $\omega_{ch} \cdot T >> 1$, i.e. the frequency bandwidth of the pulses is mainly due to the chirping (Figure 3.3.1).

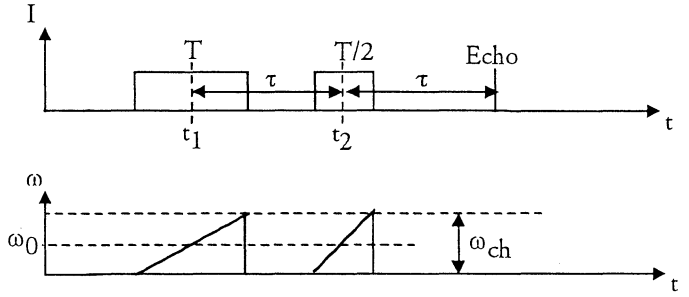

Figure 3.3.1 Two chirped square pulses give rise to a compressed signal if the chirp-rates are configured as above. This figure is essentially the same as Figure 3.1.1, apart from some extra variables that are defined.

We write the electrical field of pulse i as

$$E_i(t) = e^{-i(\omega_0 + K\cdot(t-t_i))\cdot(t-t_i)} \cdot e^{-i\bar{k}_i\cdot\bar{r}}, t \in [t_i - T_i/2, t_i + T_i/2] \,. \qquad (3.3.1)$$

As mentioned in section 3.2 the spatial factor $e^{-i\bar{k}_i\cdot\bar{r}}$ and the absolute time t_i of the pulses does not have to be included in the integral. In the following sections we will ignore the spatial part and the time of the echo and just remember that the echo will appear in the direction $\bar{k}_e = 2\bar{k}_2 - \bar{k}_1$ at time $t_e = 2t_2 - t_1$. We approximate the electrical field in the frequency domain in the way mentioned above:

$$\begin{cases} E(\omega) = 1 \; if \; \omega \in [\omega_0 - \omega_{ch}/2, \omega_0 + \omega_{ch}/2] \\ E(\omega) = 0 \; otherwise \end{cases}.$$

The solution for the photon echo

$$E_e(t) \propto \int_{\omega_0-\omega_{ch}/2}^{\omega_0+\omega_{ch}/2} e^{i\omega t} d\omega = \left[-\frac{1}{it} e^{i\omega t} \right]_{\omega_0-\omega_{ch}/2}^{\omega_0+\omega_{ch}/2} = \frac{2}{t} e^{i\omega_0 t} \sin(\frac{\omega_{ch}}{2} \cdot t) =$$

$$= e^{i\omega_0 t} \cdot \omega_{ch} \cdot \mathrm{sinc}(\frac{\omega_{ch}}{2} \cdot t)$$

(3.3.2)

Apparently the echo intensity will have the shape of a squared sinc function (Figure 3.3.2) and a FWHM that is proportional to the inverse of the chirpwidth, as was the case with gaussian pulses:

$$T_e \approx \frac{5.5}{\omega_{ch}}.$$

(3.3.3)

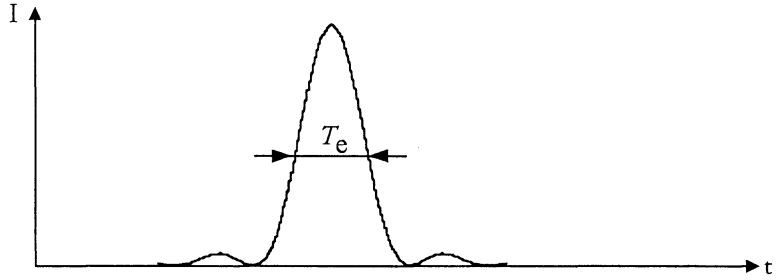

Figure 3.3.2. Intensity versus time of a photon echo pulse generated by two chirped square pulses with chirp-rates satisfying the relationship $R_1=2R_2$.

From (3.3.2) one might think that the peak value of the intensity would be proportional to the chirpwidth squared. But as we will see in the end of this section, this is not true and the reason for that is that we have normalised the electrical field in the frequency domain in Equation (3.3.2).

Later on we will look at the compression of a sequence of data bits, that is we let the first pulse consist of several pulses of length T_b. If the pulse sequence is chirped over a sufficiently large frequency interval ω_{ch}, each single bit-pulse in the sequence will interfere with the second compression pulse without interacting with any of the other bits and give rise to an echo. Then the total echo will be built up by the sum of the electrical fields from these single bits and these fields since they are all emitted at the same time when the chirp rates fulfil $R_2 = 2R_1$.

To begin with we treat the compression using a pulse of length T_b, where $T_b \leq T$, chirped over $\omega_{ch}{}^b$ and a second pulse of length $T/2$ chirped over ω_{ch}. The chirp rate over T_b is constant ($R_1 = \omega_{ch}/T$), since we have only amplitude modulated the first pulse. The result above can still be used if we chirp enough over each bit-pulse, that is if $\omega_{ch}{}^b \cdot T_b >> 1$. By replacing ω_{ch} with $\omega_{ch}{}^b$ defined as

$$\omega_{ch}^b = \frac{\omega_{ch}}{T} \cdot T_b,$$

(3.3.4)

the FWHM according to (3.3.3) is

$$T_e \approx \frac{5.5}{\omega_{ch}^b} = \frac{5.5 \cdot T}{\omega_{ch} \cdot T_b}.$$

(3.3.5)

The numerical calculation that has been done in this thesis is treated in chapter 4, but we already now mention one important result. This shows that (3.3.5) also holds when $\omega_{ch}{}^b \cdot T_b << 1$, provided that the condition $\omega_{ch} \cdot T_b >> 1$ still holds. We can understand this by assuming that the chirp over the first pulse of length T_b is negligible. In the frequency domain an unchirped pulse with length T_b is a sinc function with a FWHM of $\Delta\omega_b = 5.5/T_b$. As a result the two excitation pulses interact during a time T_I governed by the chirp of the second pulse,

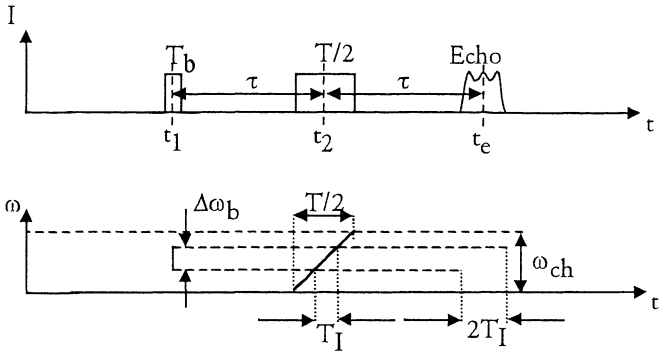

Figure 3.3.3 A schematic picture of the interaction in frequency domain between the bit-pulse and the compression pulse if $\omega_{ch}{}^b \cdot T_b << 1$. If the bit-pulse is considered unchirped the atoms will emitt radiation during a time $2T_I$ instead of at one instant and this is then the duration of the echo.

$$T_I = R_2 \cdot \Delta\omega_b = \frac{T}{2 \cdot \omega_{ch}} \cdot \Delta\omega_b,$$

(3.3.6)

that is during the time their frequencies coincide. The total echo will have a length about twice this time, $T_e = 2 \cdot T_I$, as the second chirp extends the interaction time (Figure 3.3.3) and evidentially we end up with the same result.

It has to be pointed out that no compression of the pulse T_b can be accomplished when the chirp bandwidth $\omega_{ch}{}^b$ is less than the frequency spectrum due to the length T_b. But we will later on let the first pulse be a pulse sequence of several bits of length T_b and compress that against a second pulse. In that case every bit do not have to be compressed since we want to compress a long pulse sequence of length T and this can be accomplished as long as the separate echoes all appear at the same time, that is to say that we fulfil $\omega_{ch} \cdot T_b >> 1$.

Intensity

To obtain the approximate solution for chirped square pulses we assumed that the pulses are constant and normalised in the frequency domain. By doing this we found the shape to be a sinc function and evaluated the length of the echo. If we want to calculate the intensity peak value as a function of pulse length and chirp width, as with gaussian pulses, the true constant value of the $E_k(\omega)$ functions must be known. It is easy to calculate that an unchirped square pulse of length T looks like

$$E(\omega) = T \cdot \text{sinc}\,(T(\omega + \omega_0)/2)$$

(3.3.7)

as a function of frequency and therefore the peak value is T. One can further think of a chirped pulse in the frequency domain as consisting of small unchirped pulses with different

central frequencies but the same peak value. Consequently the chirped pulse will be almost constant with this value. Let the chirped pulse have length T and bandwidth ω_{ch}. Divide the time T into N steps and let $\Delta t = T/N$. The frequency interval ω_{ch} will also be divided into N equal intervals of size $\Delta\omega = \omega_{ch} / N$, due to the linear chirp. But since we deal with small time interval Δt the smallest frequency intervals we need to consider is given by the inverse of this time-step. That is another way of saying that

$$\Delta\omega \geq 1/\Delta t \Leftrightarrow N \leq \sqrt{T \cdot \omega_{ch}} \,. \tag{3.3.8}$$

Therefore the time resolution is Fourier limited and we choose the finest resolution $\Delta t_{\min} = \sqrt{T/\omega_{ch}}$. Now let this be the constant value of the $E_k(\omega)$ functions (see Figure 3.3.4) and go back to Equation (3.3.2). It is easy to verify that the solution now reads

$$E(t) \propto e^{i\omega_0 t} \cdot \frac{T^{3/2}}{\sqrt{\omega_{ch}}} \cdot \operatorname{sinc}\left(\frac{\omega_{ch}}{2} \cdot t\right). \tag{3.3.9}$$

$$I_{peak} \propto \frac{T^3}{\omega_{ch}} \tag{3.3.10}$$

The intensity behaviour is exactly the same as for gaussian pulses (3.2.19), which might convince us that this approach is correct. Later on it will be apparent, from numerical calculations, that this is a true result.

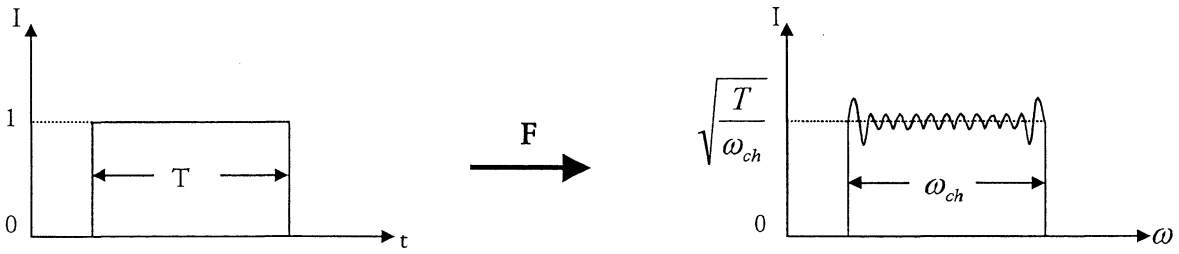

Figure 3.3.4. The Fourier transform of a normalised frequency chirped square pulse from time to frequency domain.The intensity in frequency domain approximately equals $\sqrt{T/\omega_{ch}}$. The condition $\omega_{ch} \cdot T >> 1$ is assumed to hold for the pulse.

3.4 Square pulse sequences

The results in section 3.3 can now be used to treat a compression of a sequence of data bits. For that reason consider the first pulse to be an amplitude-modulated pulse of time T, chirped over the bandwidth ω_{ch}. We assume a bit length of T_b and a constant separation between bits of length T_s (figure 3.4.1).
As has been discussed before, it is enough to consider the echo from one bit against the write pulse and then sum the electric field from all the separate echoes. Since we chirp both pulses we assume that the individual bits do not interact with each other, this is true if $T_s >> \frac{5.5 \cdot T}{\omega_{ch} T_b}$:

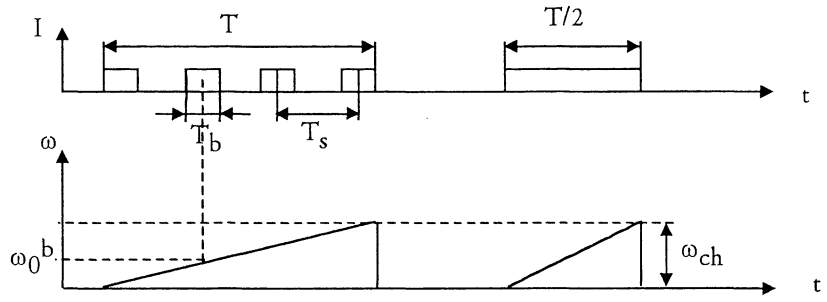

Figure 3.4.1. The input signals for the compression of a pulse sequence.

According to (3.3.9), one bit will give rise to an echo with an electrical field as:

$$E_b(t) \propto e^{i\omega_0^b t} \cdot \frac{T_b^{3/2}}{\sqrt{\omega_{ch}^b}} \cdot \mathrm{sinc}(\frac{\omega_{ch}^b}{2} \cdot t). \qquad (3.4.1)$$

All bits are chirped over an equally large frequency interval, which make $\omega_{ch}{}^b$ a constant. To calculate the total echo of the pulse sequence, we sum over all the bits.

$$E_{tot}(t) = \sum_j E_j(t) \propto \frac{T_b^{3/2}}{\sqrt{\omega_{ch}^b}} \cdot \mathrm{sinc}(\frac{\omega_{ch}^b}{2} \cdot t) \sum_j e^{i\omega_0^j t}. \qquad (3.4.2)$$

With the chirp we can express $\omega_0{}^j$ as

$$\omega_0^j = \omega_0 + \frac{\omega_{ch}^b}{T_b} \cdot T_s \cdot j, \qquad (3.4.3)$$

where ω_0 is the central frequency of the first bit. Observe that j does not have to assume every integer value in some interval, only integers that correspond to an actual bit in the stream. We can now write the intensity response as:

$$I(t) = |E_{tot}(t)|^2 \propto \frac{T_b^3}{\omega_{ch}^b} \cdot \mathrm{sinc}^2\left(\frac{\omega_{ch}^b}{2} \cdot t\right) \cdot \left| \sum_j \left(e^{i\frac{\omega_{ch}^b}{T_b} \cdot T_s \cdot t} \right)^j \right|^2 . \qquad (3.4.4)$$

Diffraction part ——▲ ▲—— Interference part

This result is important and very useful. It means that we analytically can calculate the intensity shape of the echo between an arbitrary binary sequence and a square pulse by evaluating the expression above. Expression (3.4.4) can be regarded as consisting of two different parts, we can call them the diffraction part and the interference part. The diffraction part has the same shape and intensity as the echo of one bit in the first pulse combined with the whole second pulse. This part is denoted the envelope of the echo. The interference part modulates the signal under the envelope governed by the distribution of bits in the signal. The peak electric field amplitude should be the amplitude from one bit multiplied with the number of bits, since it is inherent to the photon echo configuration that we have discussed here that the separate echoes from the bits are all in phase at $t = 0$ and add up coherently, thus we expect a N_b^2 factor enhancement of the intensity when the number of bits increase from 1 to N_b. By letting $t = 0$ and evaluating Equation (3.4.4), this statement is proved

$$I_{peak} \propto \frac{T}{\omega_{ch}} \cdot T_b^2 \cdot N_b^2 \qquad (3.4.5)$$

Equation (3.2.14) becomes particularly simple if the pulse sequence contains maximum number of bits, i.e. every position is filled. The summation index then runs from 0 to N_b-1. The sum is clearly a geometric sum and by use of Equation (A. 9) we get:

$$I(t) \propto \frac{T_b^3}{\omega_{ch}^b} \cdot \mathrm{sinc}^2\left(\frac{\omega_{ch}^b}{2} \cdot t\right) \cdot \frac{\sin^2\left(N_b \cdot \frac{\omega_{ch}^b}{2T_b} \cdot T_s \cdot t\right)}{\sin^2\left(\frac{\omega_{ch}^b}{2T_b} \cdot T_s \cdot t\right)} . \qquad (3.4.6)$$

The expression above has a striking resemblance with the intensity distribution caused by spatial inference when light is sent through multiple slits. This will be discussed briefly in section 3.9.

3.5 Decompression

We have discussed the principle of compression and we have applied that to the compression of a binary data pulse sequence. One practical use for this technique could be for high transmission rate applications in optical fibres. Imagine sending a pulse sequence trough a photon echo material, compressing it in time and then transmitting it through the fibre. This means that the signal would propagate through the fibre with a higher single-channel bit-rate than is possible with today's conventional methods, where the speed of electro-optical components set a limit for the bit-rate. But nothing is gained unless one can decompress the signal so that the electronics can handle it again after it has propagated through the fibre. That process will be discussed briefly now.
A pulse sequence of time T and a bit length of T_b is compressed by a second pulse of length $T/2$. Both pulses are chirped over the frequency interval ω_{ch}. In section 3.4 we found that the echo signal can be described by Equation (3.4.4), which has a diffraction and an interference part. The last part modulates the echo in some well-defined way while the diffraction part describes the overall spread of the echo. The time interval over which the echo is distributed is inversely proportional to the frequency chirp over one bit in the first pulse. If we want to decompress that signal, that is to restore the original sequence, all frequencies in the echo must be recorded. Accordingly, the information under the whole envelope is essential for decompression (Figure 3.5.1).

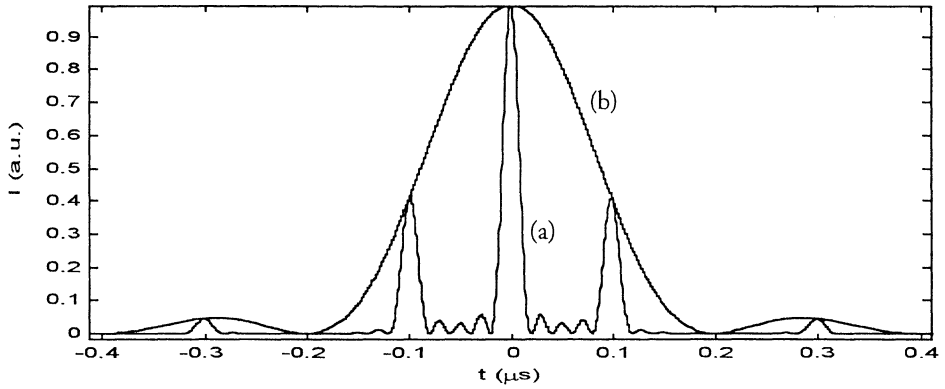

Figure 3.5.1. The line (a) is the time compression of a 5-bit pattern by a second pulse, Equation (3.4.6). While (b) describes the envelope of the signal which has the same duration as the echo between one of the bits and the write pulse, the diffraction part of Equation (3.4.4). The region under the envelope is the part required for successful decompression.

The echo is decompressed by sending it into a photon echo material followed by a second pulse of length $T/2$ and chirped over ω_{ch}. The frequencies contained in the echo (assuming compression) are simultaneously present when the pulse is interacting with the material. The situation is much the same as when we dealt with the case where the chirp over one bit was neglected (Figure 3.3.3). The second pulse will stretch the echo to the length T and the information is thus restored. If the second pulse is chirped over fewer frequencies than ω_{ch} the pulse will not be entirely restored, only a certain portion corresponding to some frequency interval in the first pulse. If the length of the pulse is not exactly $T/2$ but say T', the compressed signal will be stretched to twice this length, $2 \cdot T'$, and thus the bitrate of the outcoming signal can be choosen differently than that the originally compressed signal.

3.6 Frequency chirping

In practice it is not certain that the chirps always fulfil (3.2.14) and moreover the chirp is generated by some device that might add different kinds of non-linearity's.

Chirp-rates

If the chirp-rates do not fulfil (3.2.14) the frequency spectrum of the echo will not be emitted at only one instant. In this case we cannot find an analytic solution for the echo, but a simple model based on the principle of compression can give some hints.
Assume that the chirp-rate of the first pulse sets the requirement of the second pulse, we thus only deal with changes in the second chirp. A change of a factor k of the second chirp-rate will in practice mean a change in pulse length of the second pulse as the first pulse set the interaction interval of the frequency (below).

$$R \to R \cdot k = \frac{\omega_{ch}}{T} \cdot k = \frac{\omega_{ch}}{T/k} \ . \qquad (3.6.1)$$

If the length of the second pulse changes a factor $1/k$, the pulse is reduced by $T/2 \cdot |1/k\text{-}1|$ and the time where the echo is emitted varies with twice this time during the emission (see the schematic picture in Figure 3.1.1 to understand how a different duration of the second pulse affects the echo duration). This broadening of the echo due to a change of chirp-rate can tell something of how much the chirp-rate can be allowed to differ. A reasonable limit should be of the same order of magnitude as the echo itself, T_e. According to Equation (3.3.3) we have that

$$T|1/k_{\max} - 1| = T_e \Leftrightarrow k_{\max} = \frac{1}{1 \pm \frac{T_e}{T}} = \frac{1}{1 \pm \frac{5.5}{T \cdot \omega_{ch}}} \qquad (3.6.2)$$

Non-linearities

The frueqency chirp of the laser might also might not be a linear function but e.g. a step function if the chirp is generated by a device with a discrete time representation (se Figure 3.6.1).
If the time step is too large the signal will be made up of several distinct frequency components that are spectrally resolved. It is then obvious that the resulting echo will be made up of several echoes at different frequencies emitted at different times, creating a modulation of the echo. The criteria in order to get a compressed pulse and no modulation should be that the different frequency components in the input signals overlap. Then the Fouriertransform will more look like a perfectly chirped square signal and the previous results will still hold.
Assume that the number of steps in the chirp is Ns. Then a pulse of time T and chirped

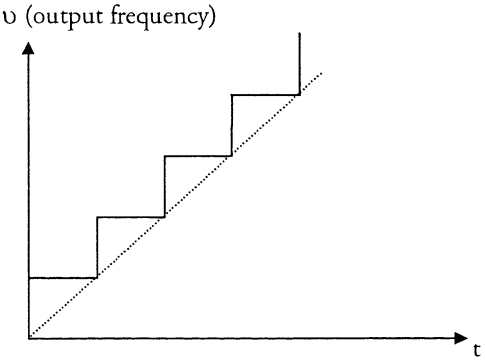

Figure 3.6.1. A chirp generated by a digital device that use a discrete time axis might look like this. The chirp consists of several frequency components.

over ω_{ch} will have Ns frequency components separated by ω_{ch}/Ns and with FWHM $5.5/(T/Ns)$ in frequency domain. We demand that the FWHM is equal to the separation, i.e.:

$$Ns = \sqrt{\frac{T \cdot \omega_{ch}}{5.5}} \qquad (3.6.3)$$

This far we have only been concerned with linear frequency chirps. It is however possible that the set-up of an experiment adds quadratic effects. Let the chirp be a quadratic function in time:

$$\omega_i(t) = \omega_0 + 2Kt + 3Lt^2 \qquad (3.6.4)$$

This is in agreement with Equation (3.2.3) that defines the linear chirp. We assume that only the first pulse has a quadratic chirp and that the second pulse has a linear chirp (see Figure 3.6.2).

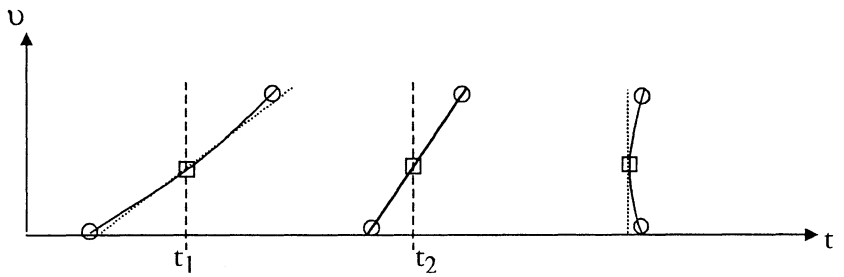

Figure 3.6.2. The first pulse has a quadratic chirp while the second pulse has a linear chirp. In this way the effects of the quadratic chirp on the echo can easily be evaluated. The figure shows how the different parts of the pulses interact and emit radiation at different times.

Since the time between the echo and the second interaction equals the time between the first and second interaction it follows that the atoms will emitt radiation at different times because of the non linear first chirp. Sections that lie symmetrically around the central time t_1 will together with pulse two cause the material to emitt radiation at the same time. Since the radiation will have two separate frequency componentes the resulting field will have a frequency that is the difference of these components, the beat frequency. The frequency of the emitted light will therefore change during the time which the echo

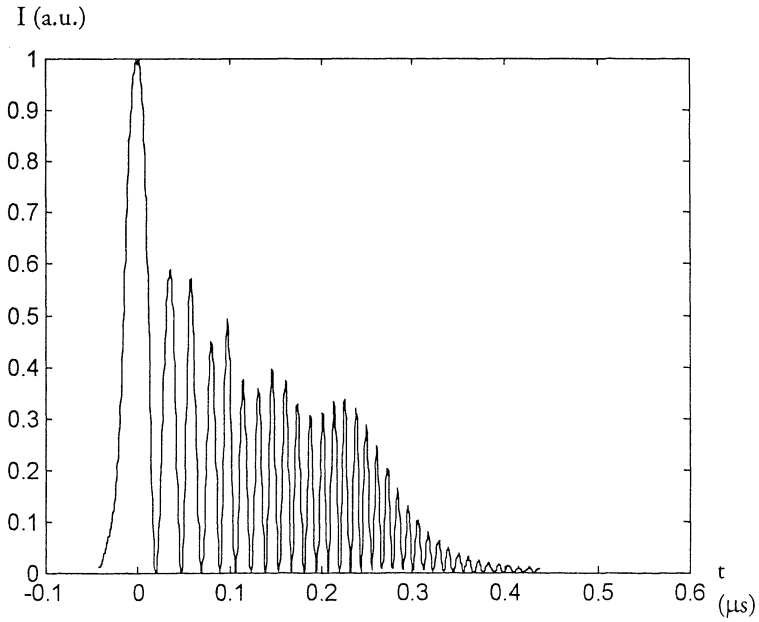

Figure 3.6.3. The echo when the first pulse has a quadratic term with constant $L = 3 \cdot 10^{11}$ Mrad/s^2.

is emitted and the echo might look like in Figure 3.6.3. The central part of the first pulse will excite many atoms that emit radiation at the same time. That is why a broad peak appears to the left. Following that peak comes several peaks with increasing frequency corresponding to the beat frequency of the two interacting components, as was explained before.
It is possible to analytically find the limit, in the value of L, when this effect starts to show. This criterion is that the quadratic chirp should not deviate more in time from the linear chirp than the FWHM of the echo from two perfect linear chirps. It is obvious that the deviation is largest at $t = \pm T/2$, where T is the pulse length. This deviation can be calculated by setting the frequencies of the linear and quadratic chirp the same and evaluate the time difference:

$$\omega_0 + 2Kt_l = \omega_0 + 2Kt_q + 3Lt_q^2$$

$$2K \cdot \Delta t = 3Lt_q^2,$$

where we have let $\Delta t = t_l - t_q$. Now set $t_q = \pm T/2$ and evaluate Δt (use Equation (3.2.4))

$$\Delta t = \frac{3}{8}\frac{L}{K}T^2 = \frac{3}{4}\frac{L}{\omega_{ch}}T^3$$

Put this equal to the FWHM of the echo

$$\frac{3}{4}\frac{L}{\omega_{ch}}T^3 = \frac{5.5}{\omega_{ch}}$$

$$L = \frac{22}{3}\frac{1}{T^3} \qquad (3.6.5)$$

If the L constant is larger than the value calculated with the above equation, several peaks will appear at different times and no compression can be accomplished.

3.7 Phase noise

Intuitively, phase fluctuations in the laser should affect the appereance of the echo if the fluctuations are large enough. The instantaneous frequency is, by definition, the derivate of the phase and large phase fluctuations will thereby cause the frequency to drift from its expected value. This means that the frequency of a chirped pulse will not really be linear in time. Instead, it will drift around the expected linear chirp.
The model that I have used is based on normal distributions. In statistics such a distribution is described by the following function:

$$N(m,\sigma)=\frac{1}{\sigma\sqrt{2\pi}}e^{-\frac{(x-m)^2}{2\sigma^2}} \qquad (3.7.1)$$

The constants σ and m are the standard deviation and expectation value, where the standard deviation is the square-root of the *variance*. It is a well-known theorem in statistics that the variance can be written as:

$$\sigma^2=\langle X^2\rangle-\langle X\rangle^2\ , \qquad (3.7.2)$$

where $\langle ...\rangle$ denotes the expectation value and X the measured quantity. If we let the quantity be the phase change after a time τ, $\Delta\phi(\tau)$, it seams reasonable that the most probable phase change is zero or that the normal distribution describing the phase change is centered around zero, i.e. $\langle\Delta\phi(\tau)\rangle=0$. According to the model used here [9], the expectation value of $\Delta\phi(\tau)$ sqaured is related to the linewidth of the laser W, measured in radians, through:

$$\langle\Delta\phi^2(\tau)\rangle=W\cdot\tau\ . \qquad (3.7.3)$$

The variance of the phase change can now be written as

$$\sigma^2=W\cdot\tau\ . \qquad (3.7.4)$$

Finally one can use a theorem stating that a normal distribution $N(m,\sigma)$ is related to the standard normal distribution $N(0,1)$ through

$$y=\frac{x-m}{\sigma}, \qquad (3.7.5)$$

where $x\in N(m,\sigma)$ and $y\in N(0,1)$. In order to sum up, the phase change after a time τ can be calculated by chosing a number, y, according to a standard normal distribution and then multiply with the standard deviation $\sigma=\sqrt{W\cdot\tau}$ to get x, which would be the phase change during a time τ from an initial value of the phase (remember that we let m = 0).

3.8 Intensity in the semi-classical model

In this section the intensity behaviour of the echo as a function of chirp width and pulse length will be obtained through an alternative approach based on a semi-classical model [1, 10].
The intensity can be defined as the number of photons per second and cross-sectional area. The number of photons emitted in a photon echo during a time T can be calculated with the following formula [11].

$$N_e = \left(\frac{N_{atoms}}{2} SL \frac{T_2^*}{T} \right)^2 TA \cdot const_{geom} \cdot \sin^2 \theta_1 \cdot \sin^4 \theta_2 \qquad (3.8.1)$$

The variables denotes the following; N_{atoms} is the density of atoms that interact with the incoming light, S is the cross-sectional area of the laser pulse, L is the length of the material, T^*_2 is the inhomogeneous broadening, T the length of the pulse and A the transition probability (Einstein coeffiecient for spontaneous emission). There is also a geometrical constant because the signal must be integrated over all angles. The excitation pulses have pulse areas:

$$\theta = \frac{2\mu T}{\hbar} E \qquad (3.8.2)$$

In this approach we assume that the pulse area is small and approximate $\sin\theta \approx \theta$. Further, divide the pulse into N small segments where the pulse is approximately unchirped (as in section 3.3 page 17). Let the duration of the pulses be T/N where $N = \sqrt{\omega_{ch} \cdot T}$ and T in Equation (3.8.1) by T/N:

$$N_e \propto \frac{N^2}{T^2} \cdot \frac{T}{N} \cdot \frac{T^2}{N^2} \cdot \frac{T^4}{N^4} = \frac{T^5}{N^5} \qquad (3.8.3)$$

We are interested in the number of photons per time, that is divide (3.8.3) with T/N:

$$I \propto \frac{T^4}{N^4} = \frac{T^4}{T^2 \cdot \omega_{ch}^2} = \frac{T^2}{\omega_{ch}^2} \qquad (3.8.4)$$

If both the pulses are of the same length, the average intensity is given by Equation (3.8.4) (since the second chirp spread out the separate echoes). In case of compression these N echoes will add up coherently, that is multiply the intensity (3.8.4) by N^2 :

$$I \propto \frac{T^2}{\omega_{ch}^2} \cdot \omega_{ch} \cdot T = \frac{T^3}{\omega_{ch}} \qquad (3.8.5)$$

We can conclude that this result agree with the ones reached with gaussian and square pulses, Equation (3.2.19) and (3.3.9). By using Equation (3.2.18) and letting $T=T_1=T_2$ and $\omega_{ch}=\omega_{ch,1}=\omega_{ch,2}$ Equation (3.8.4) can be verified for gaussian pulses.
We have seen that using a microscopic model and basically counting the number of photons emitted per second the same result can be obtained as with the Fourier based model.

3.9 Time – space duality

In section 3.3 and 3.4 we found that time compression of a single bit or a sequence of bits gives the same result as Fraunhofer diffraction in single or multiple slits. But the Fraunhofer diffraction pattern is the Fourier transform of the field distribution at the aperture through which the light is transmitted. For example, if the aperture is a square, the diffraction pattern is known to be a two-dimensional squared sinc function. On the other hand, the spatial Fourier transform of a plane wave that is constant only within the dimensions of this aperture (and zero otherwise) is also a squared sinc function. Since we here deal with processes in space we define the two-dimensional spatial Fourier transform as:

$$F(g(x,y)) = \int_{-\infty}^{\infty}\int_{-\infty}^{\infty} g(x,y)e^{-i\omega_X \cdot x}e^{-i\omega_Y \cdot y}dxdy\,, \tag{3.9.1}$$

where $\omega_{X,Y}$ are the spatial angular frequencies.
It is not obvious how to connect time-compression of a bit sequence and the Fraunhofer diffraction in multiple slits. With time-compression the diffraction pattern (the echo) can be made shorter than the original pulse, something that does not happen in ordinary spatial diffraction where the diffraction pattern always is larger then the spatial extension of the slits. An interesting question is if the time compression and spatial diffraction are two analogous phenomena that can be described with the same mathematics. To determine this we have to go a bit deeper into the topic of optics.
There are two kinds of diffraction, Fresnel (near-field) and Fraunhofer (far-field), depending on if the screen where the pattern is observed is placed close or far from the aperture. In near-field diffraction the pattern shows the shape of the aperture without distorting the picture very much, but when the screen is pulled further away from the aperture (into far-field) the pattern shows the well-known fringes of diffraction, mathematically described by a formula similar to Equation (3.4.6). It is the Fresnel number F that decide if it is Fraunhofer (F > 1) or Fresnel (F < 1) diffraction. In a recent paper published in *Optics Letters* the corresponding Fresnel number in time domain is defined as [12]

$$F = R \cdot T^2 = \frac{\omega_{ch}}{T} \cdot T^2 = \omega_{ch} \cdot T \tag{3.9.2}$$

If we compress a single pulse we demand that this number is much larger than unity, but for pulse sequence compression (consider the chirp bandwidth and length of one bit) we reach the same result if this number is greater or smaller than unity. But in order to make an analogy with Fraunhofer diffraction we always have to be in the far-field regime (F > 1). Thus there are several problems with connecting Fraunhofer diffraction to time-compression. Fourier optics can however be connected to time-compression. In this thesis there has not been enough time to investigate this connection in depth, but I will mention something about Fourier optics.
Illuminate an object, for example a square slit, with parallel light and put the object in the focal plane of a lens. The lens will decompose the light into bunches of parallel plane waves that corresponds to specific spatial frequencies in the object (or more mathematically the spatial function $g(x,y)$ describing the object). In fact, it turns out that if one put a screen at the other focal point the amplitude of the accumulated pattern is the spatial Fourier transform of the object where the spatial angular frequency quals. It is interesting to notice that since the Fraunhofer diffraction pattern due to light interference in multiple slits are the Fourier transform of the slits. If we use the slits as the object we will see the usual Fraunhofer

diffraction pattern. The diffraction pattern will be smaller than the original slits, precisely the same situation as with time-compression.
The space – time duality in photon echo processors has been observed before e.g [12] and in a paper of Kolner [13] the theory of this duality has been discussed. This subject will not be discussed anymore in this thesis, but in chapter 6 some experimental results concerning this topic will be shown.

4 Numerical calculation

4.1 Overview

The Fourier based model of the photon echo cannot be entirely evaluated by analytic calculations. That is why a numerical calculation was incorporated in this thesis. Further, effects of non-linearities and noise can best be viewed in a numerical simulation, though some results might be understood by an analytic treatment.
The numerical model takes as input the excitation pulses in the time-domain and performes the Fourier transforms to the frequency domain. The convolution is calculated. In frequency domain this corresponds to element-wise multiplication between the excitation pulses. In the last step an inverse Fourier transform, see Equation (2.3.7), gives the resulting echo.
In order to verify the various components of the computer programs one should be able to compare some calculations to known results. This was one of the reasons that the Gaussian case was worked out in detail, in section 3.2 a general solution was reached for different pulse lengths and chirp-widths. If one neglect the material constant in the Fourier model, Equation (3.2.8) is an equality not a proportionality. Thus, we can by comparing the outcome of the numerical calculation with this formula know if the result is correct.
The essential part of the calculation is made up of Fourier transforms. Numerically we deal with discrete time and frequency domains and the corresponding transform is the DFT (Discrete Fourier Transform), which under appropriate conditions can be interpreted as the discrete approximation of the continuous Fourier transform. The DFT algorithm requires that n sums of length n are evaluated, thus if we use n discrete points the work will be $O(n^2)$ arithmetic operations. In the 1960:s an enhanced algorithm for calculating the DFT was discovered, the FFT (Fast Fourier Transform) algorithm, which only require $O(n\log_2 n)$ operations, this is the algorithm being used in this thesis.
There are several possible choices of software for numerical calculations. I chose to work with the mathematical program Matlab for several reasons. It supports an internal programming language sufficient for this task, it has a FFT algorithm implemented and there are many mathematical functions for manipulating mathematical objects and present data in an easy and efficient way.

4.2 General description of the program

In Matlab the DFT and inverse DFT (fft and ifft respectively) are defined as

$$X(k)=\sum_{n=1}^{N}x(n)e^{-i2\pi(k-1)\frac{n-1}{N}},1\le k\le N \qquad (4.2.1)$$

$$x(n)=\frac{1}{N}\sum_{k=1}^{N}X(k)e^{i2\pi(k-1)\frac{n-1}{N}},1\le n\le N \qquad (4.2.2)$$

These transforms should be comparable to the analytic result reached in Chapter 3. The analytic result is of course based on the continuous Fourier transforms, which are based on integrals in time and angular frequency domain. We have to account for the continuous integration variables dt and $d\omega$ and multiply a factor 2π in Equation (4.2.2) since this is frequency domain and our analytic integration was done in angular frequency domain.
Numerically we represent the pulses as discrete vectors of length N, more accurately the time domain is sampled at N points with a distance dt between the sampling points and thus the pulse functions will also be discrete. The sampling distance $d\omega$ in the frequency domain can be related to dt by the following steps. In the theory of discrete Fourier transforms it is known that the highest possible frequency that can be represented is half the sampling frequency in time domain, that is $1/(dt\cdot 2)$. If the input vector is purely real, elements $N/2+2$ to N of the frequency vector will be the complex conjugate of elements 2 to $N/2$, the first element is the *zero frequency* (a constant function) and element $N/2$ contains the highest possible frequency (the *Nyquist frequency*). Thus the spacing should be the highest frequency divided by $N/2$:

$$d\omega=\frac{2}{dt\cdot 2\cdot N}=\frac{1}{dt\cdot N} \qquad (4.2.3)$$

It seems probable that the scale factors dt and $1/dt$ are omitted in Matlab in the definition of DFT and inverse DFT respectively. However, it is important to understand that the definitions used in Matlab still make the transforms symmetrical, that is a fft and a subsequent ifft gives the original function. The absence of these scaling factors has been verified by transforming elementary functions and compare with simple analytical results. Thus, in order to compare between numerical and analytical calculations, multiply Equation (4.2.1) with dt and Equation (4.2.2) with $2\pi/dt$.
The programs that I have made involve calculations, data interpretation and presentation of the results. Since much of the content in the programs are specific for Matlab, I will here only outline how the calculations were performed.

Create a discrete time vector t with time separation dt:

t = timevector(dt)

Create the input signals (e.g. square pulses) as a function of t, pulse length T and chirping width ω_{ch}:

*signal*1 = square(t, T_1, $\omega_{ch,1}$)
*signal*2 = square(t, T_2, $\omega_{ch,2}$)

Calculate the DFT of the input signals:

$$\mathit{fsignal1} = \mathrm{fft}(\mathit{signal1}) \cdot dt$$
$$\mathit{fsignal2} = \mathrm{fft}(\mathit{signal2}) \cdot dt$$

Calculate the frequency spectrum of the echo according to Equation (2.3.7):

$$\mathit{spectrum} = (\mathit{fsignal1})^* \cdot (\mathit{fsignal2})^2$$

Finally, calculate the inverse DFT of the spectrum to get the echo pulse as a function of time:

$$\mathit{echo} = \frac{2\pi}{dt} \cdot \mathrm{ifft}(\mathit{spectrum})$$

The steps above constitute the mathematical calculations done by the program. To make it useful for a thorough examination of the time compression, a sizeable amount of code concerning interpretation and representation of data is necessary. Many hours was also spent to make a model for chirp non-linearities and phase noise, the topic of the next section.

5 Analytical versus numerical results

In this chapter many of the results obtained in chapter 3 will be examined. Especially important is to check the pulse length and intensity behaviour of both square and gaussian pulses for different cases. Furthermore, the effects of changes in chirp-rates, non-linearities in the chirp and phase fluctuations in the laser will be examined. We start with examining the correctness of the programs.

5.1 Verification of the numerical model

As mentioned earlier the analytic result (Equations (3.2.8) and (3.2.9)) can be used to verify that the numerical programs produce the correct results. During this thesis the output from these programs have been checked against the analytic formula for a large variety of different input data. In Figure 5.1.1 one such calculation is shown and the important thing to notice here is that the relative error is small during the time when the echo pulse is large. The intensity of the pulse drop exponentially and the numerical error do not vary as much, as a result the relative error is large when the echo pulse negligible. Calculations like this was used to ascertain us that the numerical calculation was right, especially it was possible to check that the constants that were multiplied to the Matlab DFT expressions (section 4.2) were correct.

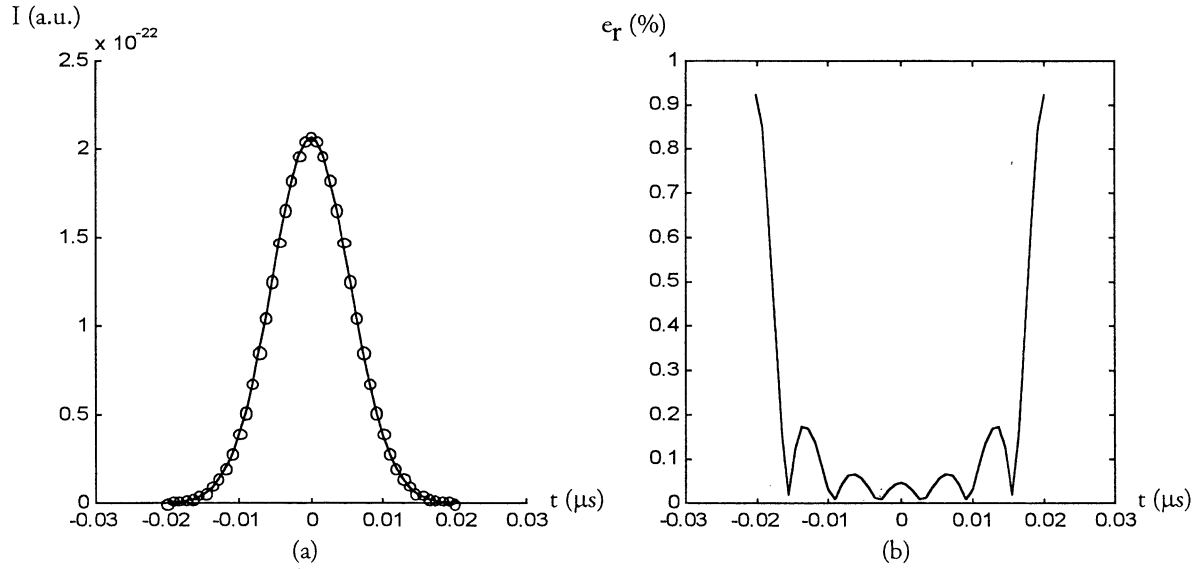

Figure 5.1.1. (a) The intensity shape of the echo resulting from two input pulses of length 10 and 5 μs, chirped over 50 MHz. The solid line is an analytic result and the circles are numerical points, they seem to be in good agreement. (b) The relative error e_r between the numeric and analytic result is small were the pulse is large. That the numerical error grows as the intensity of the pulse drops is not important since the intensity is very low in that region since we have no pulse.

5.2 The echo duration of compressed pulses

In section 3.1 we argued by a simple schematic model that the echo duration should be proportional to the inverse of the chirping width and in section 3.2 this was confirmed analytically for gaussian pulses, from Equation (3.2.15) we have $T_e \approx 4.1/\omega_{ch}$. The corresponding formula for square pulses was calculated in section 3.3, Equation (3.3.3) $T_e \approx 5.5/\omega_{ch}$. To confirm these equations a pulse (both gaussian and square) of length 10 μs were compressed by a second pulse of length 5 μs, both chirped over the same number of frequencies. The FWHM as a function of ω_{ch} is plotted in Figure 5.2.1.

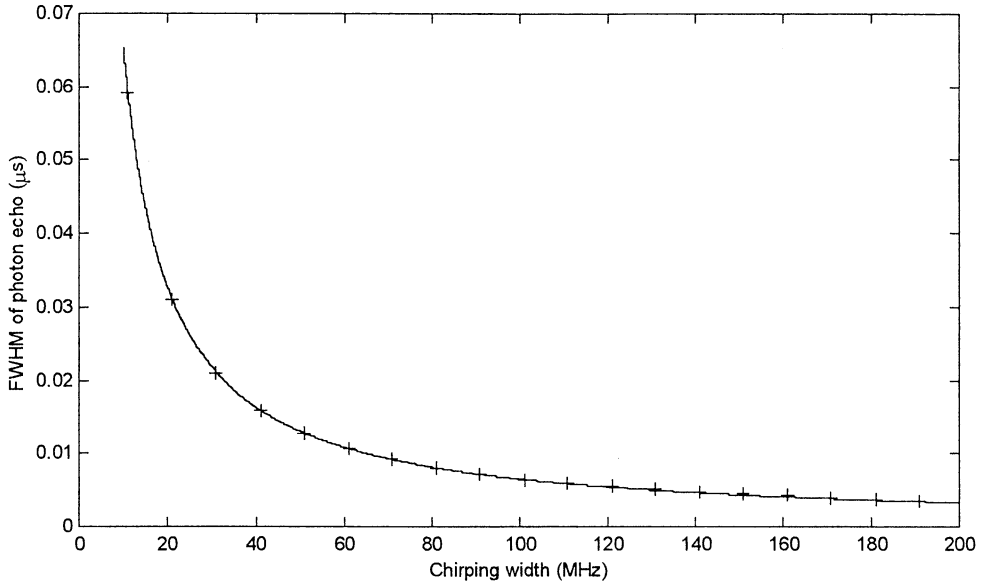

(a)

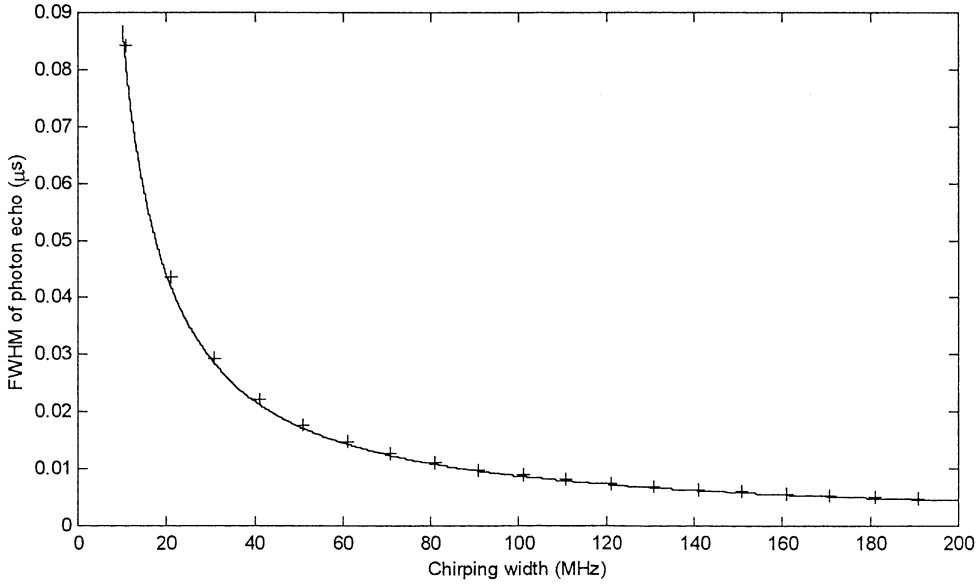

(b)

Figure 5.2.1. Echo duration as a function of ω_{ch} agree with the numerical results both for gaussian (a) and square (b) pulses (+ numerical points, solid line analytic curve). In both cases $T \cdot \omega_{ch} >> 1$ is fulfilled for all the pulses.

In section 3.3 the echo between two square pulses of length T_b and $T/2$ chirped over $\omega_{ch}{}^b$ and ω_{ch} respectively, were $\omega_{ch}^b = \omega_{ch} \cdot T_b / T$, were studied in both the regimes $\omega_{ch}{}^b \cdot T_b >> 1$ and $\omega_{ch}{}^b \cdot T_b << 1$. The FWHM is the same in both cases, Equation (3.3.5) shows that $T_e = 5.5 \cdot T/\omega_{ch} \cdot T_b$ approximately (see Figure 5.2.2).

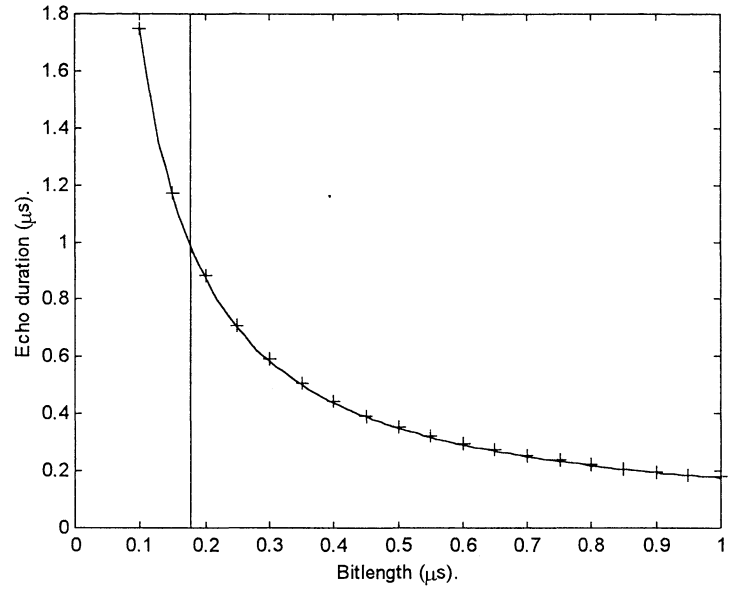

(a)

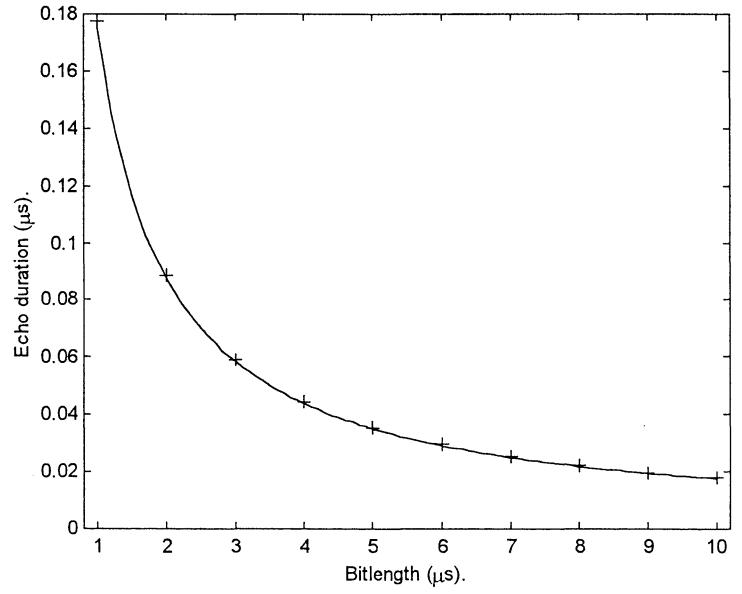

(b)

Figure 5.2.2. Pulse echo FWHM as a function of bitlength for square pulses. Clearly the result holds in both the regimes $\omega_{ch}{}^b \cdot T_b >> 1$ and $\omega_{ch}{}^b \cdot T_b << 1$. (The solid vertical line in (a) shows where $\omega_{ch}{}^b \cdot T_b = 1$.)

5.3 The intensity of compressed pulses

In Chapter 3 it was shown that the peak intensity is inversely proportional to the chirping width and cubic in the pulse length for single bit compression, this is true both for gaussian and square pulses, Equations (3.2.19) and (3.3.10) respectively. Both these expressions describe how the peak intensity vary with the pulse length T and the chirp width ω_{ch}, all constants have been disregarded in the treatment. It is then not possible to compare absolute values between numerical and analytical results, since the numerical calculation solve Equation (2.3.7) fully. Equation (3.3.10) has been verified by doing least linear square fits of the numerical points with the peak intensity as the free variable, see Figure 5.3.1 below.

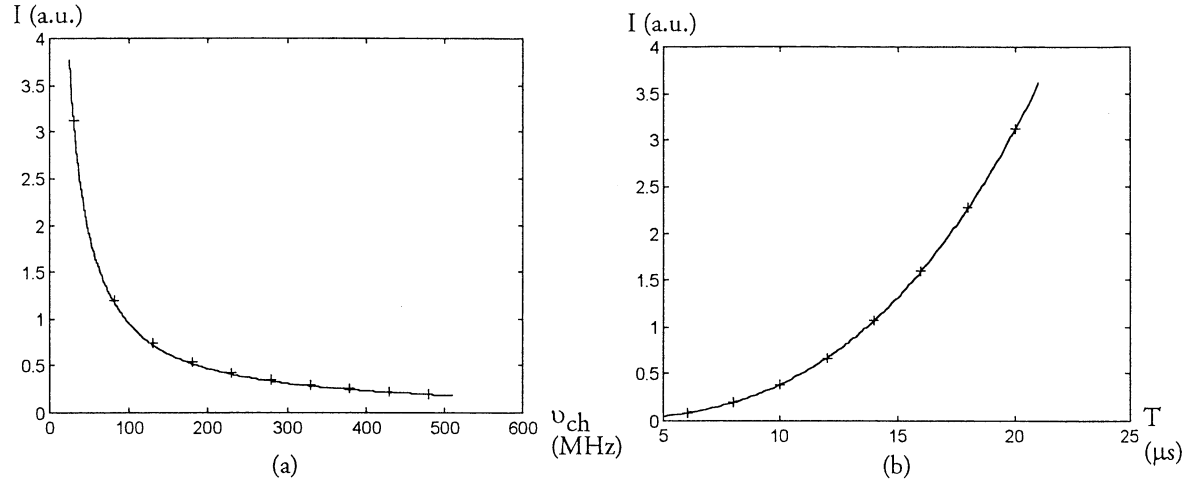

Figure 5.3.1. In the plots above the crosses (+) are numerically calculated values, while the solid lines are fitted to these data by a linear least square fit method. As can be seen, the intensity as a function of chirp width (a) and as a function of pulse length (b) agree very well to the analytic result.

Equation (3.4.5) shows that for pulse sequence compression, the intensity is quadratic in the number of bits, a result of the coherence in the photon echo process. In Figure 5.3.2 the intensity as a function of the number of bits is plotted. The pulse sequence of 5 bits is chirped over 250 MHz during 10μs and the bit length is held constant at 1μs.

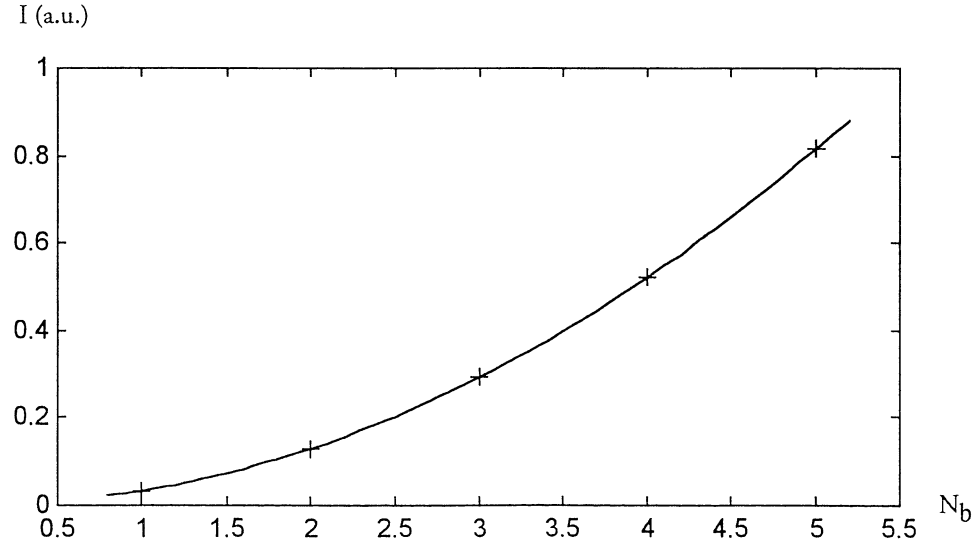

Figure 5.3.2. The crosses (+) are numerical points and the solid line is a least linear square fit of these points. The intensity is quadratic in the number of bits, N_b.

5.4 The effect on the echo duration from non ideal frequency chirps

In section 3.2 we found that a requirement for compression is that the chirp over the second pulse is twice as fast as the chirp over the first pulse, Equation (3.2.14). Numerical calculations have shown that the echo duration is very sensitive to how the chirps are arranged relative too each other. Figure 5.4.1 below show how much the echo is broadened if the second chirp-rate is 0.5 % larger than the 500 MHz that is required for compression.

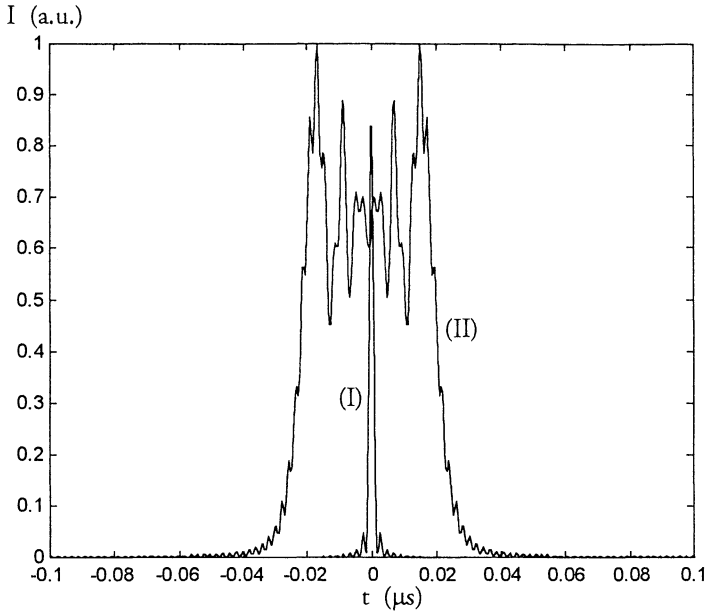

Figure 5.4.1. The brief signal (I) is the echo from a 10μs and 5μs pulse, both chirped over 500 MHz. If the second pulse is chirped over a larger frequency interval, in this case 0.5 % larger, the echo will have a considerably longer duration (II). The ratio between the duration of the longer and shorter pulse is 22.

In section 3.6 the sensitivity of the chirp-rates was treated with a simple model based on the time during which the echo was emitted (in a simplified model for compression the echo is emitted at one instant but broadened in time because it has a finite frequency spectrum). The factor k that the second chirp-rate R_2 is allowed to change with can be calculated by Equation (3.6.2), $R_2 \rightarrow k \cdot R_2$. This was reached by saying that the echo is allowed to be emitted during a time that is equal to the duration of the echo at compression. That this is a reasonable model can be checked by calculating how much the echo would broaden if the time during which the echo is emitted is set to ten times the echo duration instead (see the discussion that lead to Equation (3.6.2)), Figure 5.4.2.

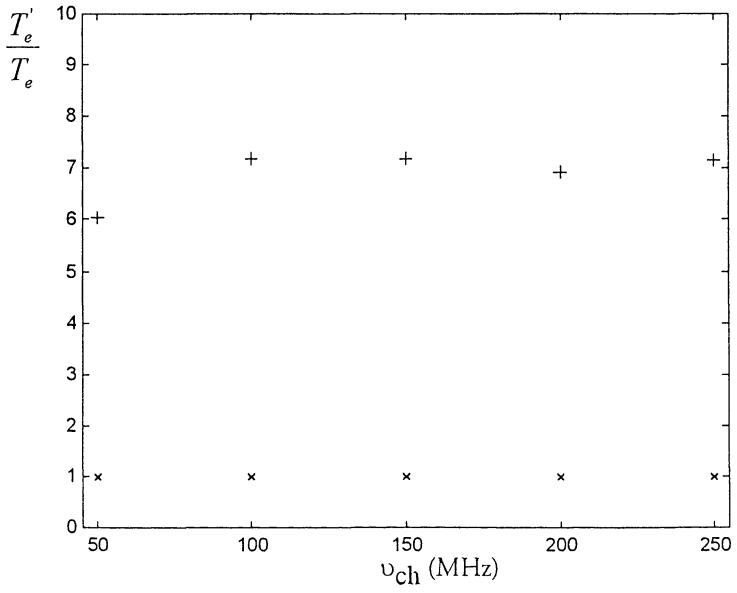

Figure 5.4.2. T_e is the echo duration at optimal compression and T_e' the echo duration when the second chirp-rate is multiplied with some factor. When this factor is calculated by Equation (3.6.2), the ratio T_e' / T_e is one, no broadening occur (x). If the factor is calculated to broaden the echo to ten times T_e instead, a broadening roughly ten times can be seen (+). This shows that the simple model in section 3.6 is reasonable.

In practice the chirp might be generated by some digital function generator that use a discrete time function. The chirp will not be a linear function but a step function (see Figure 5.4.3), the effects of such a chirp will be investigated now. Numerically this is done by setting a chirp that is a step function and perform a piecewise integration in order to calculate the phase.
In section 3.6 we reached the conclusion that the number of sampling points in the signal generated by the digital function generator have to exceed a certain value given by Equation (3.6.3) for the echo to be unaffected by the discretisation of the chirp. Numerical calculations have shown this to be a good criterion. Figure 5.4.3 show two calculations where the number of sampling points used were more and less than the criteria and how this affects the echo.

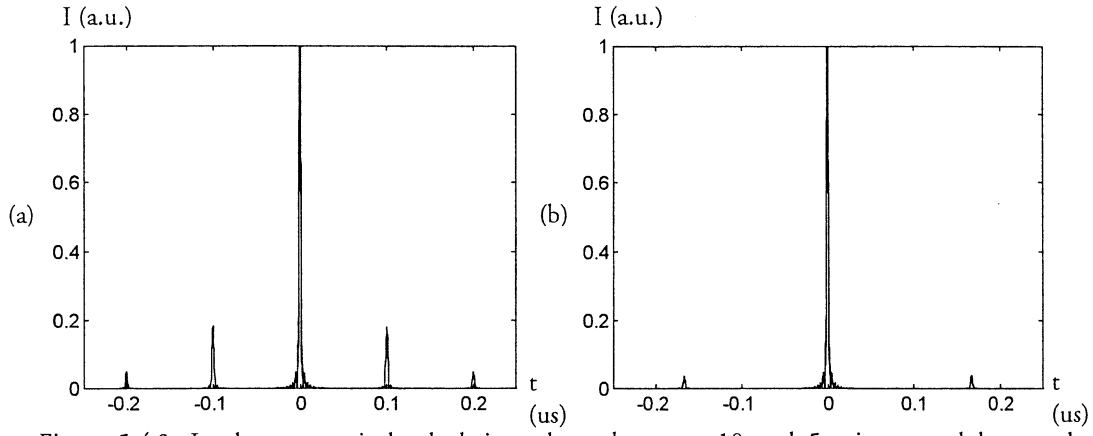

Figure 5.4.3. In these numerical calculations the pulses were 10 and 5 microsecond long and frequency chirped over 300 MHz. According to Equation (3.6.3) the number of sampling points, *Ns*, should be 40 for the shorter pulse (we chose twice as many sampling points for the longer pulse so that they both have the same time step). In (a) Ns_1 = 60 and Ns_2 = 30 and the echo is clearly modulated, in (b) Ns_1 = 100 and Ns_2 = 50 and the echo shows no modulation and has the same FWHM as a perfectly compressed echo.

We conclude this section with two simulations where the first pulse has a quadratic chirp and the second one a linear chirp. In section 3.6 a criterion when the quadratic term do not affect the output echo was reached and this has proven to be a good guideline in the simulations done. In Figure 5.4.4 two calculations with different quadratic terms are shown and these support Equation (3.6.5) .

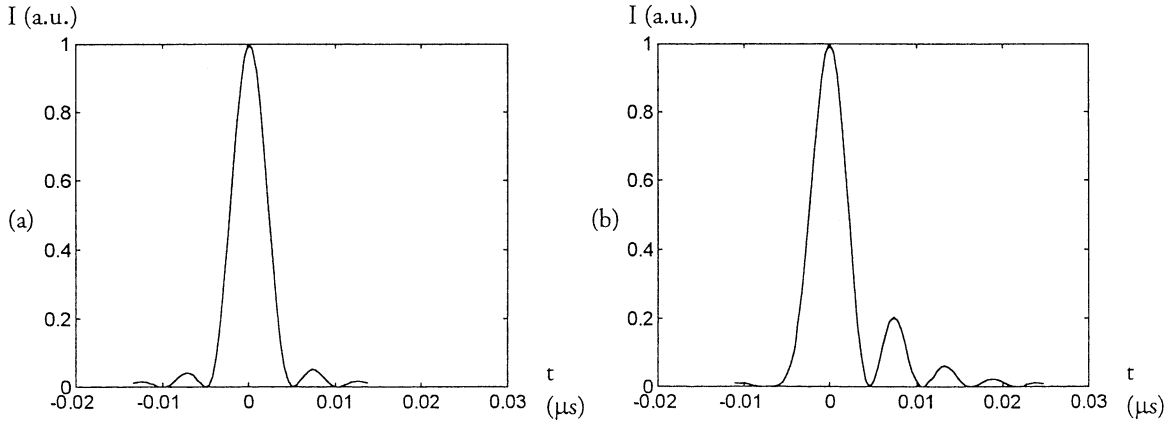

Figure 5.4.4. In the above simulations the pulses had a duration of 10 and 5 microseconds and they were chirped over 200 MHz. The chirp over the first pulse had a quadratic term $3L \cdot t^2$ and according to Equation (3.6.5) this term will start affect the appearance of the echo if $L > 7 \cdot 10^9$ Mrad/s^2. In (a) and (b) the constant L is set to $1 \cdot 10^9$ Mrad/s^2 and $20 \cdot 10^9$ Mrad/s^2 respectivly.

5.5 Phase noise

Based on the earlier work that has been done on compression in this group it was suggested that the stability of the laser, together with large frequency chirps, are of great importance to achieve high compression. One of the goals of this thesis was to implement a numerical model for phase noise and evaluate how sensitive the echo duration is to phase fluctuations.
The phase noise model was implemented in the following way. At every N_p sampling point a random phase factor is chosen according to the model described in detail in section 3.7. This factor is a function of the laser linewidth and the time interval between every point. It is then added to the accumulated phase drift since the phase has a memory. In total the pulse is sampled with N, $N_p < N$, points and in order to make the phase drift a smooth curve a spline method was used to interpolate between these points. Numerically the phase is represented with a discrete vector of length N, a perfect linearly chirped pulse with no phase fluctuations change phase quadratically in time. The phase noise vector was superimposed on this vector to give the total phase as a function of time. In Figure 5.5.1 the phase drift and the frequency of a simulated pulse with 10-microsecond duration chirped over 100 MHz is shown.

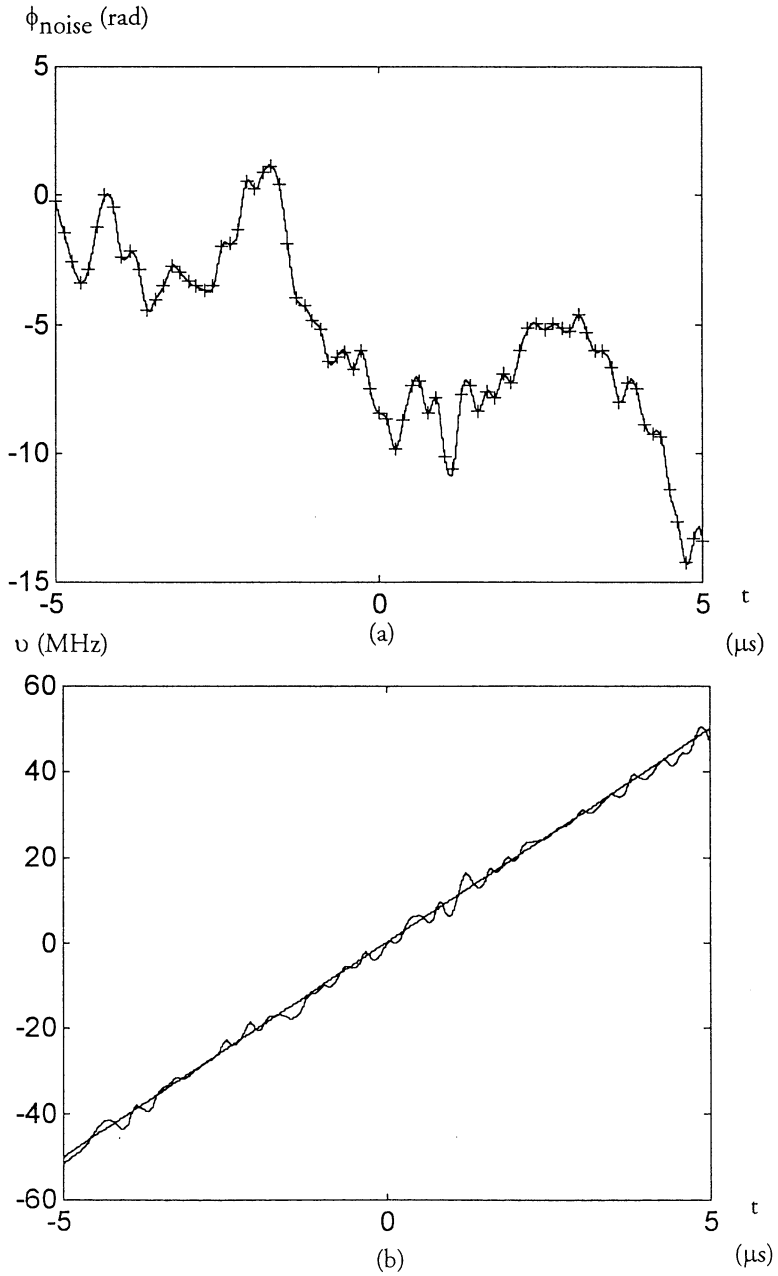

Figure 5.5.1. In this figure the phase drift and the resulting frequency is plotted. In this calculation the laser linewidth has been set to 1 MHz to make the fluctuations larger and more clear. In (a) one can see how the phase noise is interpolated between the points were a new random phase factor is calculated. The number of points have in this case been chosen as $N_p = \sqrt{\omega_{ch} \cdot T}$ (Equation (3.3.8)). Plot (b) is a differentiation of the total phase and as can be seen the freqeuncy is not linear in time because of the phase noise.

Experimental work conducted by Wang [14] parallel to this theoretical work gave the opportunity to compare my theoretical calculations with her experimental results. In some of the measurements the width of the echo was several times larger than predicted by theory and we believed for some time that a phase noise model might explain this broadening. However, the numerical simulations when a phase noise model was implemented were unable to explain this discrepancy. The experimental echoes were rather smoothly broadened compared to the analytically calculated echoes, while the phase noise model produced several peaks spread over a large time interval (see Figure 5.5.2). Still, the results from the simulations seamed reasonable to us considering the model that we used. Since the frequency is drifting from its linear value (see Figure 5.5.1) it is probable that the interaction time with atoms at different resonance frequencies will vary. The echo will consist of several distinct frequency components randomly spread over the chirping interval ω_{ch}, in contrast to a perfectly compressed echo when the frequency spectrum is constant within the chirping interval (remember that we set the Fourier transform of the input pulses as constant in section 3.3). These frequency components have random phase relationships and will thereby randomly interfere, at some times constructively and at other times destructively producing an intensity spectrum like in Figure 5.5.2.

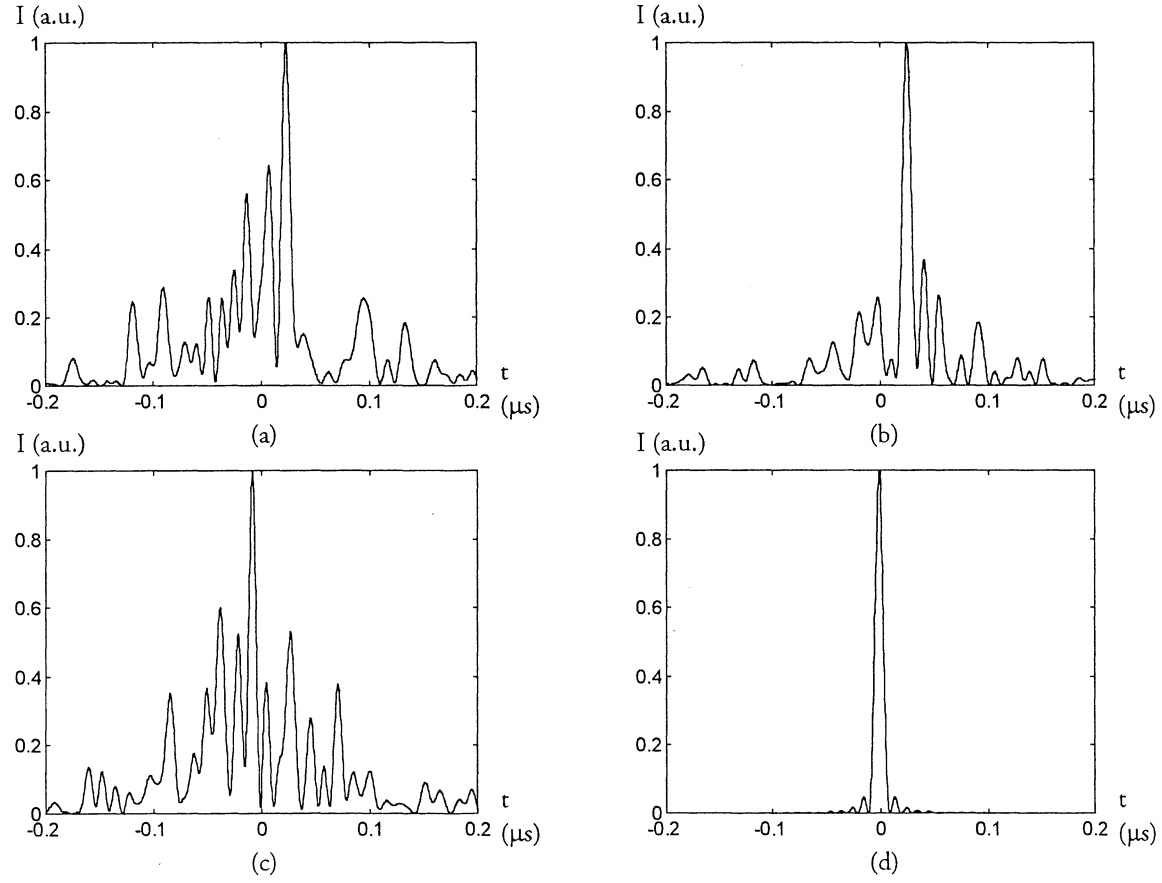

Figure 5.5.2. The first three plots above (a,b,c) are numerical simulations with a phase model implemented, the linewidth was set to 300 kHz, as is described in this section while (d) is a perfectly compressed pulse. The input pulses were 10 and 5 microsecond long chirped over 100 MHz. The number of sampling points were approximatly $N_1 \approx 21\,000$ and $N_2 \approx 10\,000$. In order to evaluate how the output echo is affected by how often a phase change is applied the number of phase changes N_p was different in the plots (a,b,c) above. This number was chosen according to: (a) $N_p \approx N_{1,2}/3$, (b) $N_p \approx N_{1,2}/100$ and (c) $N_p \approx \sqrt{(\omega_{ch} \cdot T_{1,2})}$. No significant difference can be observed between plots (a,b,c) but the frequency fluctuations of the input pulses were considerably different. When N_p is high, e.g. in (a), the frequency can take a jump of tens of megahertz over a nanosecond timescale which do not seam reasonable. It seams that a more physically correct choise should be as in (c) (see Figure 5.5.1), where the frequency fluctuations are smaller and smoother.

The intensity spectrum of an echo when the phase model is applied can be compared to that of a laser with several equally spaced frequency modes with random phase relation [15]. The intensity spectrum recorded over some time interval is very similar to the results from the simulations, which have convinced us that the output is consistent with the model used. However, experimentally these kinds of echoes have not been observed which they should have if the model was correct. I suspect that the linewidth comes into the calculation in a wrong way, resulting in a frequency drift that is too large for that linewidth. To summarise it seems as if the model is not entirely correct but implemented in a right way.

5.6 Compression and Decompression

In this chapter the goal has been to numerically verify as much as possible of the analytical results obtained in chapter 3. The last part of this chapter will show the total concept, from compression of an arbitrary pulse sequence to the decompressed echo. In section 3.4 an analytic treatment of the echo shape when an arbitrary pulse sequence is compressed gave Equation (3.4.4). In the figure below a complete calculation is done, that means a compression of a pulse sequence and a decompression of the relevant part of the compressed echo (see section 3.5 for a discussion of how much of the echo is needed for a successful decompression). From the plot in Figure 5.6.1 one can see that Equation (3.4.4) describes the substructure completely which supports the approach in the analytical treatment. The decompression of only a part of the compressed echo that is twice as large in time as the FWHM of the envelope shows that this information is sufficient for reproducing the input pulse sequence. Further simulations have shown that using a smaller part of the echo gives to strong a distorsion of the pulse sequence.

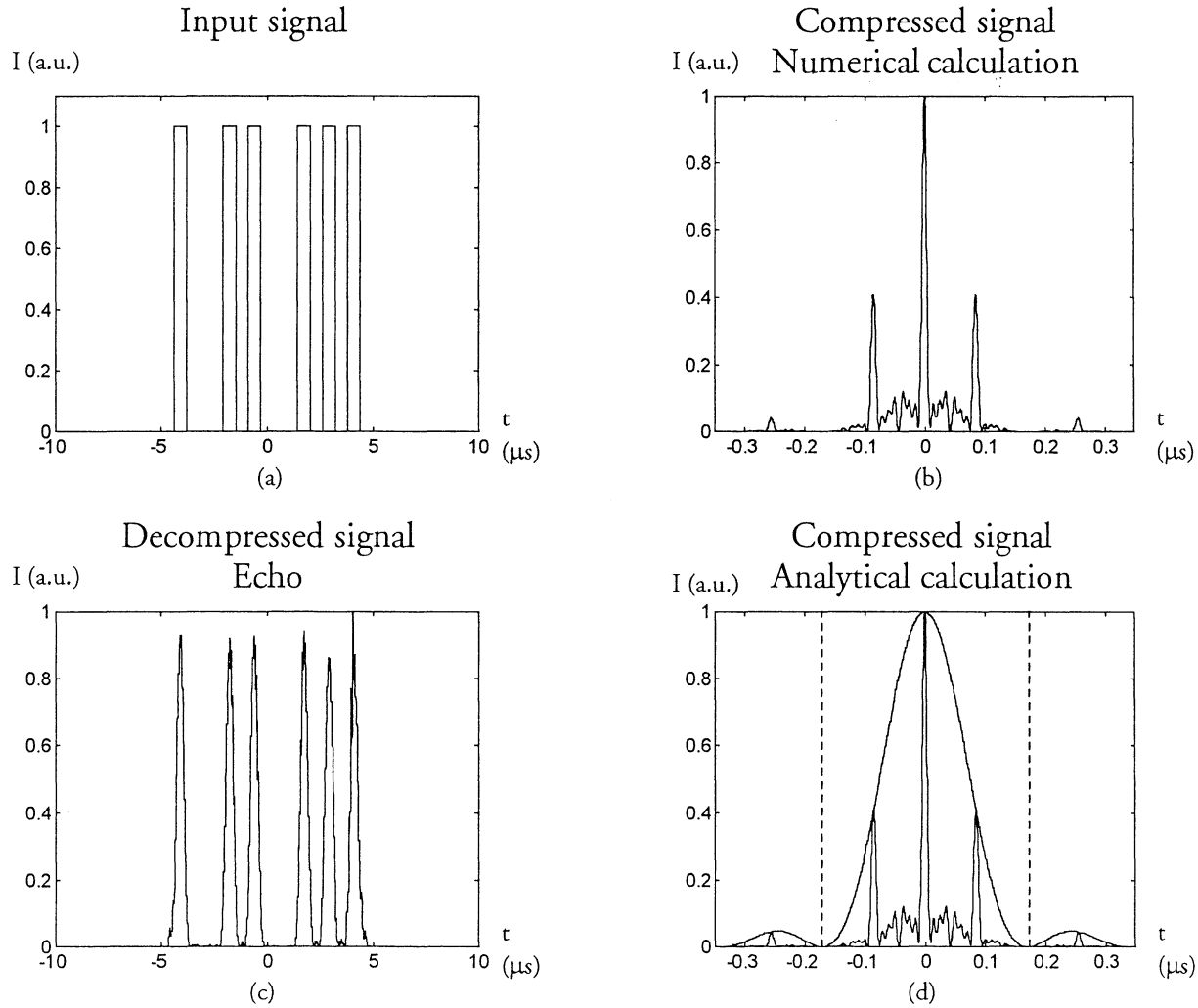

Figure 5.6.1. The above plots show a compression of a pulse sequency (a) and a subsequent decompression (c) of the compressed echo (b,d). In (b) and (d) the numerical and analytical calculations (see Equation) of the same input pulses are shown and as can be seen they agree very well. The part of the compressed echo that was used in the decompression process is indicated by the dashed lines in plot (d), this interval corresponds to twice the FWHM of the envelope. That we only use a finite part of the pulse makes the decompressed bits look more smooth since we loose the high frequency components that build up the sharp edges of the square pulses.

6 Experimental results

The experiments done by Wang [14] made it possible to immediately test the ideas experimentally. In the following sections some of the results from the measurements will be shown and compared to the theory.
The most important parts of the set-up is the fast chirping diode laser built in this group and the photon echo material. This material is a YAG crystal doped with trivalent rare earth ion Tm^{3+} that has a transition line at 793.1 nm. In order to increase the phase memory time the crystal was cooled down to about 4° K in a cryostat.
The echo was recorded by a photo multiplier and then sent to an oscilloscope where one could chose to record a single echo, single-shot mode, or average over several recorded echoes, average mode. After a while a problem with the average measurement mode was discovered. Because of the set-up the triggering time of the oscilloscope varied between recorded echoes and thereby the echoes used in average data were not recorded at the same time, we call this time gitter. In some of the measurements single-shot echoes were recorded to remove this time gitter that, for example, could destroy the substructure in the echo of a compressed pulse sequence. The measurement mode will be indicated when it is of importance.

6.1 Duration of compressed pulses and pulse sequences

One of the main goals with the experiments was to compress a signal as much as possible and compare the echo duration with the theoretical value. The echo durations of the best such measurement is tabulated in Table 6.1.1. From this data it can be seen that the best achieved degree of compression is 450 times, more specificly from 10 μs to 22.1 ns. These echoes were recorded as single echoes on the oscilloscope and then averaged on a computer (7 single echoes for every chirp range) to remove the time gitter effect but improve the signal-to-noise relative to the single-shot measurement. However, there is still a large discrepancy between the theory and experiment, a factor of about 7 that evidently is independent of the chirp width. We have not yet been able to explain this. One idea we had was that phase fluctuations broaden the peak but numerical simulations could not support this idea (see section 5.5). Another possibility is that the chirp rates did not fulfil the condition of compression, Equation (3.2.14), that would broaden the echoes. More experiments are probably needed to find an explanation for this deviation.

υ_{ch} (MHz)	T_{exp} (ns)	T_{theory} (ns)	T_{exp} / T_{theory}
23	236	38.1	6.2
46	118	19.1	6.2
69	60	12.7	4.7
84	61.6	10.5	5.9
115	59.3	7.63	7.8
161	28.7	5.45	5.3
230	22.1	3.81	5.8

Table 6.1.1. The input pulses in the experiment described above were 10 and 5 μs long. The highest compression achieved here is one order of magnitude better than what has previously been published [4,3,2]. But the constant discrepancy between theory and experiment has to be explained and for that better measurements have to be performed.

The best achieved degree of compression of a pulse sequence is about 100 times, from 20 μs to 212 ns, when the input pulses were 20 an 10 μs, the bit length 1.34 μs and the bit separation 2.19 μs. Each of the input pulses were chirped over 650 MHz in this

measurement. All the echoes from this pulse sequence compression experiment were averaged on the oscilloscope, which makes it hard to compare the obtained results with the theory because of the time gitter. In section 6.3 an experiment better suited for comparision with theory is discussed.
We were also interested in measuring the FWHM of the envelope when a pulse sequence is compressed. This is possible by removing all but one bit in the sequence and perform a compression. The best results were obtained when the bit length was set to 0.91 μs and the second pulse to 7 μs. In Figure 6.1.1 the echo duration as a function of time is plotted and as can be seen this measurement is more consistent with the theory. The fact that the pulse length and chirp width over the bit are so small in comparison with the data in Table 6.1.1 might explain why the experiment and theory agree reasonably well in Figure 6.1.1 but not in Table 6.1.1.

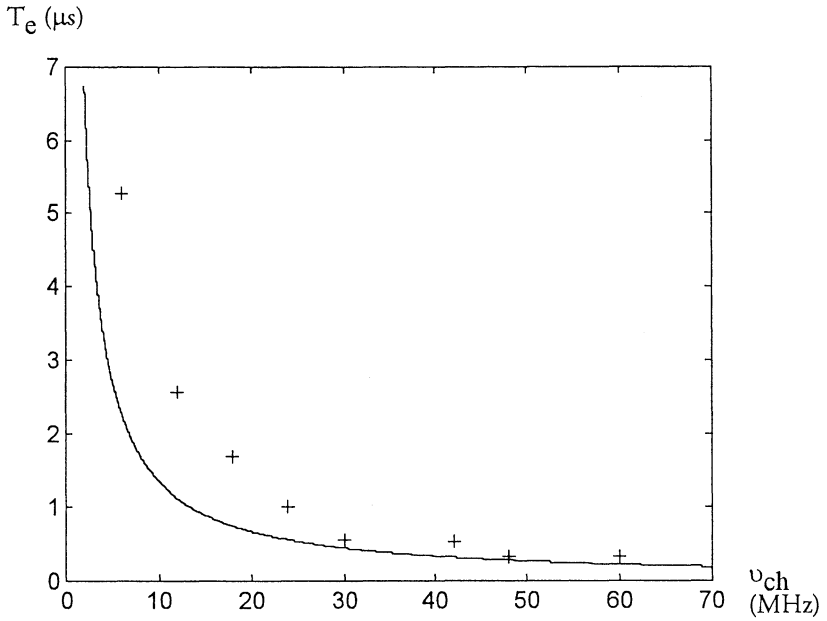

Figure 6.1.1. When only one bit in a sequence is compressed the experimental durations (+) are almost consistent with the theoretically calculated curve. The deviation is getting larger when the echo duration is comparable to or longer than the original bit length. At higher compression the agreement is better.

6.2 Peak intensity of the compressed pulses

In section 3.3 we found that the peak intensity should be inversely proportional to the chirping width and cubic in the pulse length, Equation (3.3.10). That is if the pulse length is kept constant the recorded intensity should be inversely proportional to ω_{ch}.
The experimental peak intensities in Figure 6.2.1 were measured on echoes recorded in average mode on the oscilloscope. The input pulse durations were set to 10 and 5 microseconds respectively. The experimental data points fit better to an $1/\omega_{ch}^2$ curve than to a $1/\omega_{ch}$ curve, i.e. the peak intensity drops more rapidly with the chirping width than what is expected. This might be a result of the averaging, since the magnitude of the time gitter does not change with ω_{ch} but the echoes that are averaged get more narrow with larger chirps. A better way of doing it would be to measure the peak intensity of the single echoes, to avoid the triggering problem on the oscilloscope.

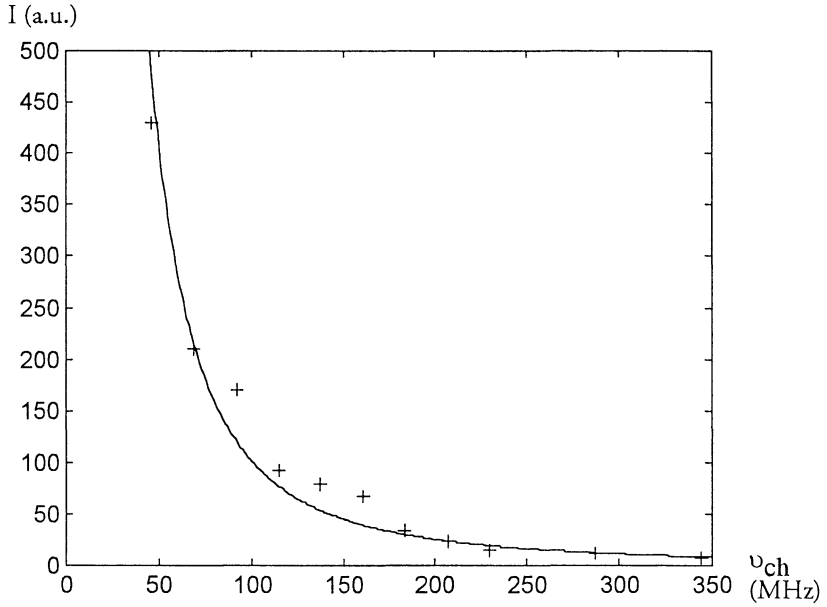

Figure 6.2.1. The experimentally measured peak intensities fit to an inverse quadratic function, not to an inverse function as the theory predicts. It is possible that an experiment when the peak intensity of single echoes, instead of averaged echos, is measured would fit better to an inverse function as discussed in the text.

6.3 Observed substructure of compressed pulse sequences

In the high compression measurements of pulse sequences that was discussed in section 6.1, no substructure could be observed. Therefore single echoes were recorded of less compressed sequences with fewer bits in order to increase the signal strength and make the substructure more evident. In Figure 6.3.1 two echoes with observable substructure are plotted.

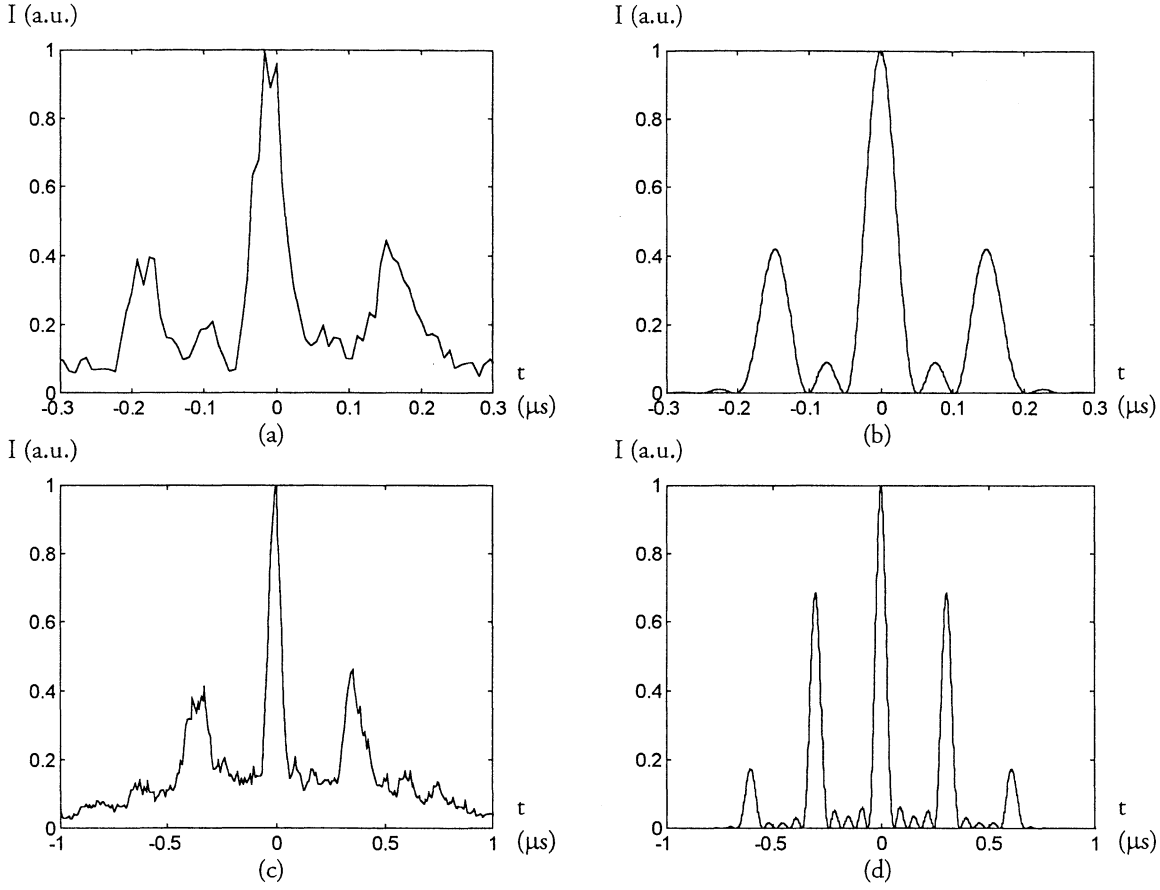

In plot (a) the intensity spectrum of the echo is shown when a pulse sequence of 3 bits chirped over 70 Mhz during 21.4 μs was compressed. The bitlength is 1 μs and the bit separation 2 μs. In (b) the analytically calculated echo is plotted and clearly the substructure is reproduced, although the noise blurs the finest structure somewhat. This becomes worse in plot (c) where the number of bits has been increased to 5. The bitlength is 2/3 μs, the separation time 2 μs and the chirp width 35 MHz. A theoretical plot (d) shows fine substructure that has been washed out in the experimental data. It is obvious that a better signal-to-noise ratio is needed to get the complete information.

The results above have convinced us that the theory is capable of reproducing the experimentally seen substructure, but it is also evident that the signal-to-noise ratio has to be improved to see the finest substructure when the number of bits is increased. An interesting continuation of this work could be to numerically evaluate what signal-to-noise ratio is required to be able to decompress the echo successfully.

7 Conclusions & Comments

One of the goals with this diploma work was to investigate the practical limits of pulse compression using photon echoes, especially interesting is how non-linearities and noise limit the degree of compression.
A first step was to do an analytical treatment of the compression process and to use the results when building numerical programs. In a first step, the integral describing the photon echo was solved exactly under the assumption that the input pulses are gaussian shaped in time. Square pulses are more frequently used in experiments but analytically it is easier to deal with gaussian pulses.
It was a hope in the beginning of my work that the compression of square pulses and pulse sequences also could be solved analytically or at least that an approximate solution could be found. A possible approach had been suggested in a paper published in Optics Letters that led to an approximate solution for single square pulse compression. Using this idea I reached expressions for the echo duration and peak intensity. I used the same approach to treat compression of arbitrary pulse sequences. I found that in the special case when the time separation between the bits is constant, the intensity pattern of the echo is completely analogous to the intensity spectrum observed in the famous Fraunhoufer diffraction experiment in multiple slits. The echo is modulated under an envelope and the modulation is determined by the time separation between the bits and the bit length. It is the envelope that decides the spread of the echo and this envelope has the same shape as an echo between one of the bits in the pulse sequence and the second pulse. For arbitrary pulse sequences, the FWHM of the envelope is approximately $5.5 \cdot T/(\omega_{ch} \cdot T_b)$, where T is the total pulse length, ω_{ch} the chirp during this time and T_b the bit length. For a successful decompression at a later stage, the echo has to be recorded during a time given by twice the FWHM of the envelope. This very reasonable conclusion is supported by numerical calculations. The peak intensity of the echo is proportional to $T/\omega_{ch} \cdot T_b^2 \cdot N_b^2$, where N_b is the number of bits in the pulse sequence. That is, dense pulse sequences are preferred from a signal strength point of view since the intensity is quadratic in the number of bits.
With an explicit expression of the electric field for the general photon echo, not necessarily compression, when the input pulses are gaussian in time, a numerical model was built. To ensure the correctness of this model, the analytical and numerical calculations were compared. It was then an easy task to switch to square pulses instead, since the foundation of the calculations is independent of the input pulses. The purpose of a numerical model was to investigate how different non-linearities in the chirps and phase noise in the laser affect the compressed echo. Another advantage was that many aspects of the compression process could be investigated thoroughly before attempting to explain the resulting echo with an analytical model
An interesting question is how the echo duration changes if the second chirp-rate is not precisely twice as fast as the first one. It was found that the echo duration is very sensitive to a deviation from the correct alignment of the chirps. The second chirp-rate can only be allowed to deviate from its supposed value by a factor k given by Equation (3.6.2).
I also investigated how discrete frequency chirps affect the echo. If the time interval between the discrete points is too large, the frequency spectrum of the echo will consist of several frequency components and the intensity spectrum will be modulated. The number of points in the discrete representation of the pulses should be larger than the value calculated with Equation (3.6.3) in order to avoid a modulation of the echo. The echo duration would also change if the chirps are not linear, e.g. if a quadratic term is added to the chirps. The effect of a quadratic frequency chirp on one of the pulses was investigated. If the quadratic term is too large, Equation (3.6.5), the echo will consist of one strong peak and several weaker peaks appearing with increasing (decreasing) frequency after (before) the strong peak.

It has been suggested that a laser with high frequency-stability is necessary in order to achieve high degree of compression and one of the goals with this diploma work was to implement a model for phase fluctuations and then investigate how the echo duration is affected by the linewidth of the laser. If the linewidth is chosen large enough, the numerical calculations show echoes with several peaks spread over a large time interval. This pattern is probably due to interference between several distinct frequency components with random phase relationships. In the lab, there has been no observation of such echoes which the numerical simulations suggest when the linewidth is set to one of the laser in the experiment (300 kHz short-time linewidth). One possibility is that the model is incorrect and then no conclusions can be made from these simulations. Another possibility is that the model is correct in the sense that large frequency fluctuations would give an echo as in the simulations. Then the problem might be that the linewidth in the calculations gives frequency fluctuations larger than the real frequency drift of the laser or that the measured linewidth is not only a result of phase fluctuations in the laser. A possible conclusion could then be that the linewidth does not affect the compression since such echoes have not been observed experimentally. I any case, phase fluctuations and their effect on the echo have to be investigated further.

With the experiments conducted by Wang [14] I was able to continuously compare my theoretical results to her experimental data. The ratio between the experimental and theoretical echo durations for single pulse compression turned out to be 7 in one experiment. We have not been able to find a trustworthy explanation for this discrepancy. In another experiment a single bit in a pulse sequence was compressed, the goal was to observe the envelope and measure the FWHM. In these experiments however the measured echo duration agreed reasonably well with the theory. In the latter experiment the bit-length and chirp width were considerably shorter than in the former which might be an explanation for the better agreement in this case.

In an attempt to observe the substructure or modulation of the echo from a compressed pulse sequence, two sequences containing three and five bits were compressed. The substructure was observable in both experiments. Here there was a good agreement with the theory. The experiment with less number of bits had the best agreement with the theory. That is because the substructure becomes finer when the number of bits is increased and to observe the full substructure requires a better signal-to-noise ratio.

The peak intensity was also measured experimentally for different chirp widths. These measurements did not show the behaviour that we expected, the peak intensity was inversely proportional to the square of the chirp width while we expected it to be inversely proportional to the chirp width. We identified a problem with the synchronisation of the oscilloscope trigger that made these experimental values unsuitable for a comparison with the theory. New experiments are required to check the theoretical result.

In many of the measurements the recorded echo was an average of several echoes and it was only in a late stage of the experiments that we realised the problem with the triggering time of the oscilloscope. Many of the measurements were not comparable with the theory as a result. It is of importance to avoid this problem and to do more experiments on single pulse compression with large frequency chirps, in order to understand why the experimental durations of the echoes were 7 times larger than theoretically predicted. In this context it might be a good idea to check how good the chirp-rates fulfil the condition for optimal compression. The frequency stability of the laser and the noise that is responsible for the measured linewidth of 300 kHz should, if possible, be investigated in-depth.

It is possible to connect the numerical calculations and the experiments more deeply. E.g. a pulse sequence can be compressed on a computer, then synthesised with a digital function generator and decompressed in an experiment. In this way, the decompression process can experimentally be investigated before a fibre amplifier is developed. It can also be useful to record the phase, along with the intensity, of an experimentally compressed pulse sequence. A

Fourier transform of the signal will show the original pulse sequence. This might be an easy way to investigate if the signal-to-noise ratio of the set-up is good enough to do a decompression of that signal for a specific number of bits. With the possibility to record the phase information and to synthesise signals many interesting experiments can be envisioned, especially before a working fibre amplifier has been developed.

Acknowledgements

I would like to thank everyone in the Photon Echo group that have helped me in some way during the time this diploma work has been going on. Especially I want to thank the following people.

My supervisor Stefan Kröll for giving me the opportunity to take part of the work that has been done in this group. His great commitment and experience have helped me a lot and been a constant source of inspiration.

Nicklas Ohlsson, whose room I intruded, for always answering my questions and also for many interesting discussions about physics and other things.

Xiangjun Wang for an interesting and rewarding co-operation (thank you for experimentally confirm some of my results).

Krishna Mohan has been a very interesting acquaintance with whom I have had many nice discussions, not only about physics.

To everyone else in the Atomic Physics Division that I have disturbed from time to time, thank you.

I also want to thank my family for supporting me during all my years at the university, especially this last half a year.

Finally I want to thank my girlfriend Céline for making this summer and autumn so very special.

Appendix A

Definition of Fourier transform

$$F[f(t)] = \int_{-\infty}^{\infty} f(t) \cdot e^{-i\omega t} dt \tag{A. 1}$$

Definition of inverse Fourier transform

$$F^{-1}[g(\omega)] = \int_{-\infty}^{\infty} g(\omega) \cdot e^{i\omega t} d\omega \tag{A. 2}$$

Useful relationships

$$F[f(t \pm t_0)] = e^{\pm i t_0 \omega} F[f(t)] \tag{A. 3}$$

$$F^{-1}[g(\omega \pm \omega_0)] = e^{\mp i \omega_0 t} F^{-1}[g(\omega)] \tag{A. 4}$$

$$F\left[e^{\pm i \omega_0 t} f(t)\right] = \left(F[f(t)]\right)(\omega \mp \omega_0) \tag{A. 5}$$

$$F^{-1}\left[e^{\pm i \omega t_0} g(\omega)\right] = \left(F^{-1}[g(\omega)]\right)(t \pm t_0) \tag{A. 6}$$

Integrals

$$F\left[e^{-zt^2}\right] = \sqrt{\frac{\pi}{z}} e^{-\omega^2/4z}, \text{ if } \mathrm{Re}[z] > 0 \tag{A. 7}$$

$$F^{-1}\left[e^{-z\omega^2}\right] = \sqrt{\frac{\pi}{z}} e^{-t^2/4z}, \text{ if } \mathrm{Re}[z] > 0 \tag{A. 8}$$

Evaluation of the geometric sum $\sum_{j=0}^{n-1} \left(e^{ix}\right)^j$:

$$\sum_{j=0}^{n-1} \left(e^{ix}\right)^j = \frac{\left(e^{ix}\right)^n - 1}{e^{ix} - 1} = \frac{e^{ixn/2}\left(e^{ixn/2} - e^{-ixn/2}\right)}{e^{ix/2}\left(e^{ix/2} - e^{-ix/2}\right)} = e^{ix(n-1)/2} \frac{\sin\left(xn/2\right)}{\sin\left(x/2\right)}. \tag{A. 9}$$

References

[1] I. D. Abella, A. Kurmit, and S. R. Hartman, *Photon Echoes*, Phys. Rev., **141**, 391 (1966)

[2] Felix R. Graf, Bernd H. Plagemann, Eric S. Maniloff, Stefan B. Altner, Alois Renn, and Urs. P. Wild, *Data compression in frequency-selective materials using frequency-swept excitation pulses*, Optics Letters, **21**, 284 (1996).

[3] T. Wang, H. Lin, and T. W. Mossberg, *Optical bit-rate conversion and bit-stream time reversal by the use of swept-carrier frequency-selective optical data storage teqniques*, Optics Lettres, **20**, 2033 (1995)

[4] Y. S. Bai and T. W. Mossberg, *Experimental studies of photon-echo pulse compression*, Optics Letters, **11**, 30 (1986)

[5] Y. S. Bai and T. W. Mossberg, *Photon echo optical pulse compression*, Appl. Phys. Lett., **45**, 1269 (1984)

[6] A V Durrant, J Manners and P M Clark, *Understanding optical echoes using Schrödinger's equation: I. Echoes excited by two optical pulses*, Eur. J. Phys., **10**, 291 (1989).

[7] Ulf Elman, *Ivestigations of issues relevant to the application of photon echoes in information technology*, Ph. D. thesis, Lund Institute of Technology, 1998.

[8] W. R. Babbitt, *The Response of Inhomogeneously Broadened Optical Absorbers to Temporally Complex Light Pulses*, Ph. D. thesis, Harvard University, 1987

[9] Tetsuhiko Ikegami, Shoichi Sudo, and Yoshihisa Sakai, *Frequency Stabilization of Semiconductor Laser Diodes*, MA: Artech House, 1995

[10] R. H. Dicke, *Coherence in Spontaneous Radiation Processes*, Phys. Rev., **93**, 99 (1954)

[11] R. Krishna Mohan, Baozhu Luo, and Stefan Kröll, *Delayed single-photon self-interference*, Phys. Rev. A, **58**, 1 (1998)

[12] Loïc Ménager, Ivan Lorgeré, Jean-Louis Le Gouët, R. Krishna Mohan, and Stefan Kröll, *Time-domain Fresnel-to-Fraunhofer diffraction with photon echoes,* Optics Letters, **24**, 927 (1999).

[13] Brian H. Kolner, *Space-Time Duality and the Theory of Temporal Imaging*, IEEE J. Quantum Electron, **30**, 1951 (1994).

[14] Xiangjun Wang, *Photon-echo based Optical Data Compression Using an External Cavity Diode Laser*, Master thesis, Lund Institute of Technology, 2000

[15] L. A. Westling and M. G. Raymer, *Intensity autocorrelation measurements and spontaneous FM phase locking in a multi-mode pulsed dye laser*, J. Opt. Soc. Am., B **3**, 911 (1986)